Fabrication and Characterization of Self-Assembled Tissue Rings using Patient Cells with Variants in Aneurysm Genes

Maters Thesis - Hande Eyisoylu

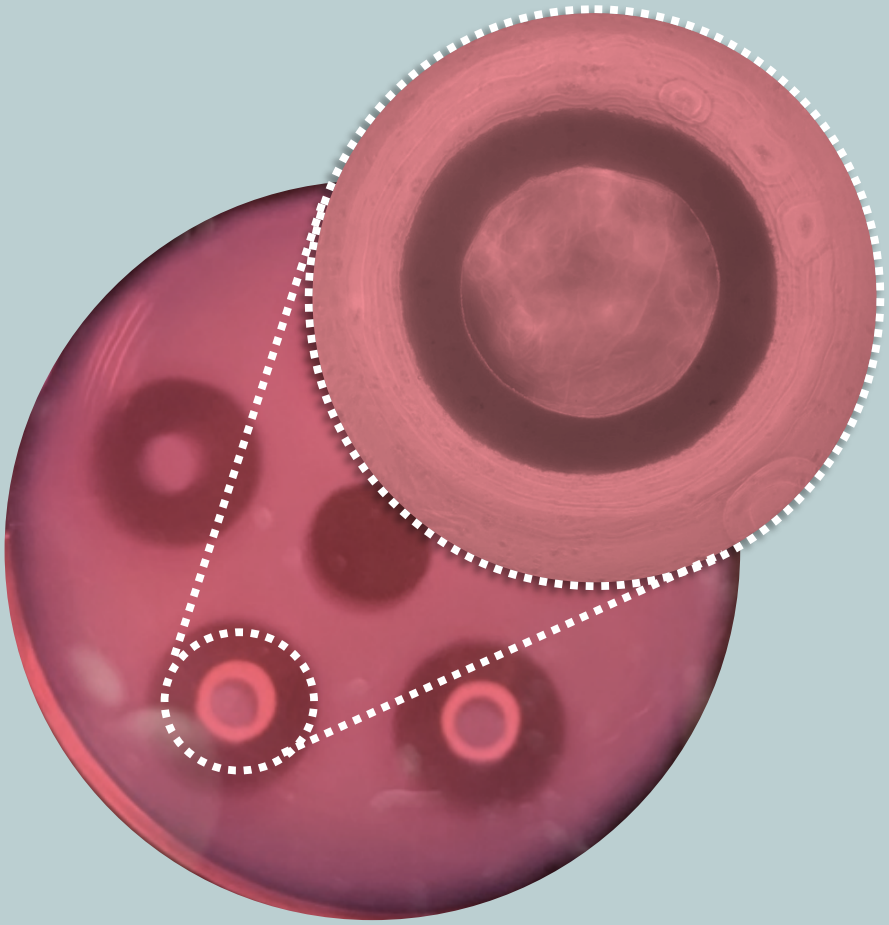

TU Delft

Erasmus MC
Universitair Medisch Centrum Rotterdam

Fabrication and Characterization of Self-Assembled Tissue Rings using Patient Cells with Variants in Aneurysm Genes.

Towards the Development of an In-Vitro Model of an Abdominal Aortic Aneurysm

by

Hande Eyisoylu

to obtain the degree of Master of Science
at the Delft University of Technology,
to be defended publicly on Thursday, November 28th, 2019.

Student number: 4694007
Supervisors: Dr. Heleen van Beusekom (Erasmus MC)
Dr. Danielle Majoor-Krakauer (Erasmus MC)
Dr. Arne Ijpma (Erasmus MC)

Dr. ir. Lidy Fratila-Apachitei (TU Delft)
Prof. Dr. ir. Amir A. Zadpoor (TU Delft)

An electronic version of this thesis is available at `http://repository.tudelft.nl/`.

TU Delft

Acknowledgements

The completion of this project was possible with the contributions of many people around me. I am grateful for their continuous support and guidance throughout the project. It would not have been possible to learn so much without the continuous support and valuable advices of my supervisors Dr. Heleen van Beusekom, Dr. Danielle Majoor-Krakauer and Dr. Arne Ijpma at Erasmus Medical Center. I am thankful for the opportunity to learn so much during this study not just regarding the project but about research in general. I would like to especially thank my supervisors for making my thesis project not just educational but enjoyable and interesting during our weekly discussions. I am also grateful for the support and guidance of Dr. Lidy Fratila-Apachitei at TU Delft, throughout the process of writing my thesis.

My special thanks to Maria Alves for patiently training me in the lab and her help throughout the project. I would like to thank Robert Beurskens, Michiel Manten and Amal Mansoor for their help regarding mechanical testing equipment and Joke Pola-Knook for her help in overcoming the difficulties with cell culture.

Finally I would like to thank my family for always being supportive and understanding throughout my studies abroad. I am extremely grateful for their support and sacrifices. Their encouragement, love and acceptance has been the driving force making it possible for me to complete my studies and become the person I am today.

Hande Eyisoylu
Delft, November 2019

Contents

List of Abbreviations

AAA	Abdominal Aortic Aneurysm
ECM	Extracellular Matrix
TGFβ	Transforming Growth Factor Beta
TGFBR2	Transforming Growth Factor Beta receptor type 2
COL3A1	Collagen Type III alpha 1 chain
DMEM	Dulbecco's Modified Eagles Media
FBS	Fetal Bovine Serum
PBS	Phosphate Buffer Saline
PDMS	Polydimethylsiloxane
ABS	Acrylonitrile butadiene styrene
CAD	Computer Aided Design
PFA	Paraformaldehyde
PSR	Picrosirius Red
H&E	Hematoxylin and Eosin
SMC	Smooth Muscle Cells
MSC	Mesenchymal Stem Cells

Abstract

Aortic Abdominal Aneurysm (AAA) is a chronic degenerative disease of the arterial wall. The aortic vessel wall abnormally dilates due to multiple possible causes and may eventually rupture [1]. It is characterized by several factors leading to the extreme dilation due to the degeneration of the vessel wall extracellular matrix (ECM). It is often asymptomatic making it difficult to diagnose before rupture [2, 3]. The etiology of AAA is complex and not yet fully understood. Hallmarks of the disease are; loss of elastin and vascular smooth muscle cells, influx of inflammatory cells which produce proteases, increased stiffness due to higher collagen content, disturbed ECM network organization and an eventual destruction of the ECM leading to the vessel rupture [2, 4]. These changes may be related to environmental factors in combination with a genetic susceptibility, or by major defects in genes involved in the ECM homeostasis. Family history and genetic conditions play an important role in aneurysms. In approximately 20 % of aneurysm patients there is a familial disease or a family history of aneurysms, and in these families a major genetic defect is to be expected. Aneurysm patients show pathogenic variants in less than 5 % of the screened patients however, variants of unknown clinical significance in aneurysm genes occur at a much higher frequency. To determine the effect of these variants in aneurysm genes, functional assays which display a change in the function of the gene product needs to be established. Tissue engineering, in recent years, have become an alternative approach to animal models in developing tissue repair/replacement grafts or disease models [5]. For this study, a cell-derived self-assembly tissue ring culture method was chosen and optimized for the use of patient cells with different pathogenic variants in aneurysm genes. After optimizing the culture conditions, the ring formation and structural ECM characteristics were compared for patient and control cases. The kinetics of ring formation showed differences in behavior and speed for patient and control cell lines. Patient lines took longer to settle into the ring shape and contract to their final thickness. The incidence of ring failure was higher in patient cases. The final patient rings were significantly thinner and non-uniform, additionally they showed a significantly lower area fraction of collagen compared to the controls. The tissue rings could not be mechanically tested due to their fragility. However, it was possible to identify the structural differences between the patient and control cases which were expected due to the pathogenic variants in the aneurysm genes of these patients. With further improvements, this method could be a potential functional assay for revealing the effects of variants of unknown significance in aneurysm genes, waiting to be identified.

1

Introduction

1.1. Background on Aortic Abdominal Aneurysm (AAA)

Aortic Abdominal Aneurysm (AAA) is a chronic degenerative disease of the arterial wall, where the vessel wall abnormally dilates due to multiple possible causes and may eventually rupture [1]. Figure 1.1 compares a healthy sized aorta to the dilated aneurysmal aortas in the thoracic and abdominal regions. It is characterized by several factors leading to the extreme dilation of the arterial wall due to the degeneration of the arterial wall extracellular matrix (ECM). AAA affects 2-10% of the elderly population and has a higher than 80% morbidity rate when left untreated [2, 4, 6]. It is often asymptomatic making it difficult to diagnose before rupture [2, 3]. Additionally, with an aging population the incidence of AAA is on the rise [7]. The etiology of AAA is complex and not yet fully understood. The hallmarks of the disease are; loss of elastin and vascular smooth muscle cells, influx of inflammatory cells which produce proteases, increased stiffness due to higher collagen content, disturbed ECM network organization and eventually destruction of the ECM leading to the vessel rupture [2, 4]. These changes may be related to environmental exposure (like smoking) and mechanical stress (hypertension), possibly in combination with a genetic susceptibility, or by major defects in genes involved in the ECM homeostasis. The latter are referred to as aneurysm genes [7].

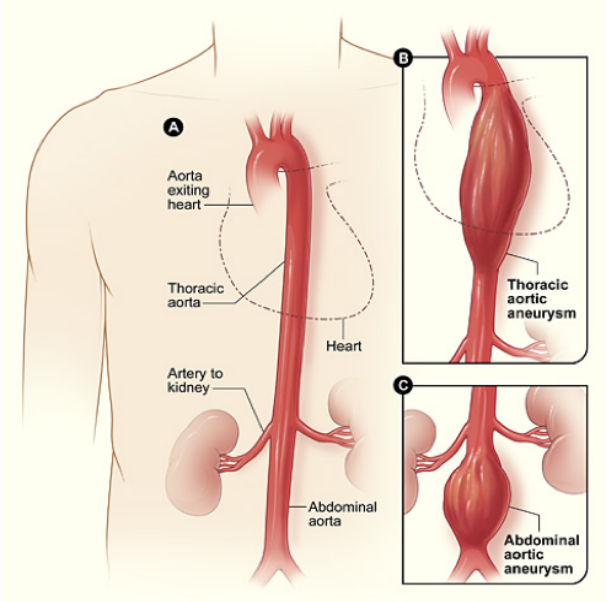

Figure 1.1: A) The figure shows a healthy aorta, the thoracic and abdominal regions are indicated with the arrows. Figure B and C show what a dilated aorta, an aneurysm at the thoracic and abdominal regions look like.

Aortic aneurysms occur most commonly in the abdominal region. This, can be explained by the fact that the abdominal region of the aorta contains less elastin compared to the regions closer to the heart [2]. Elastin and collagen are the essential structural proteins responsible from mechanical strength, elasticity and the structural integrity of blood vessels. These fibrous proteins of the ECM give the aorta its ability to resist plastic deformations against high pressures while providing mechanical strength [4, 6]. Arterial wall structure is made up of three layers with distinct composition; tunica adventitia, tunica media and tunica intima. Adventitia is the outermost layer composed of fibroblast cells, which play an important role in ECM remodeling, and bundles of type I collagen fibers. This collagen rich layer provides tensile strength and resist rupturing during high pressures. Tunica media, found between adventitia and intima, is mainly composed of lamellar elastin fibers integrated with collagen fibers and layers of smooth muscle cells [2, 8]. 70% of the collagen in the media layer is of type III while 30% is type I[8, 9]. The vessel wall ECM is a dynamic structure which undergoes constant remodeling where ECM producing cells like fibroblasts and smooth muscle cells play an important role [8, 9]. In the case of a diseased aorta this organizational structure is lost and the ECM homeostasis can no longer be maintained. Which results in an aorta which can no longer function efficiently.

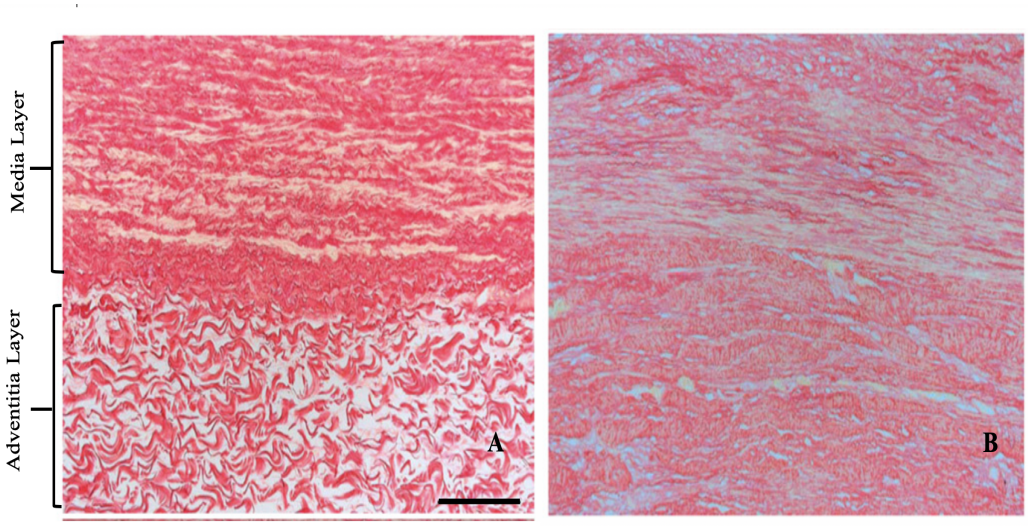

Figure 1.2: A) A healthy aortic tissue, stained for collagen using Picrosirius Red. The distinction between adventitia and the media layers may easily be seen by the organizational differences. B) An aneurysmal tissue from an AAA patient similarly stained, the organizational differences can not be distinguished between the two layers. The ECM organization has been altered, in turn affecting the functional properties of the vessel wall[4].

Figure 1.2 compares the healthy aorta (A) and an aneurysmal aorta (B) stained to specifically show the collagen in the tissue [4]. While there is a clear distinction in the organization of collagen in the adventitial and the medial layers of the vessel wall in the case of the the healthy aorta, this distinction is lost in the aneurysmsal case. Tissue samples harvested from aneurysmal aortas at the advanced stages of the disease, reveal the loss of these structural proteins and their fibrous network. A compensatory deposition of collagen is often observed in aneurysmal tissue along with a loss of elastin. In addition to the changes in the ECM organization, the matrix degrading enzymes produced by inflammation and oxidative stress lead to a further destruction of the ECM proteins. It is not only the loss of ECM fibers but also the changes in their organizational structure that affects the vessel wall strength[1]. An inability to form the interconnected network in which collagen fibers are naturally organized, could prevent the external mechanical loads from being uniformly distributed across the entire vessel wall [1, 3]. The healthy artery which is normally able to accommodate stress and blood flow can no longer effectively function or maintain its structure as the remodeling and organization of the ECM is impaired [1].

While the exact initiation and development mechanisms of the disease are unknown, the risk factors include atherosclerosis, hypertension, smoking, male sex, advanced age, genetic conditions and family history [1]. Alterations to the ECM structure may be due to; defects in genes affecting connective tissue, environmental factors, increased wall stresses and impaired remodeling for compensation as well as degeneration of the ECM [1, 7]. Mutations in genes leading to connective tissue disorders can be reasons for aneurysm formation in younger patients. Some connective tissue disorders such as Marfan, Loeys Dietz, and Ehlers-Danlos syndrome show increased risk of aortic pathologies. Defects in the aneurysm genes which are responsible from collagen production, crosslinking and the regulation of TGFβ signaling may be some of the underlying reasons predisposing patients to aneurysm formation. [10–12].

1.2. Clinical significance and the genetics of AAA

It is important to be able to identify individuals and their family members who are at risk of developing aneurysm for early detection and intervention. Family history and genetic conditions play an important role in aneurysms [10, 11]. In approximately 20 % of aneurysm patients there is a familial disease or a family history of aneurysms, and in these families a major genetic defect is to be expected. However, current DNA analysis of aneurysm patient identifies pathogenic defects in less than 5 % of the screened patients [12]. Indicating that many aneurysm genes are still unknown. Some defects in known aneurysms are classified as variants of unknown significance, because functional evidence of specific variants in these aneurysm genes is lacking. Finding the genetic cause (mutation) in a family is important since it may convey information about the severity of the disease and guide clinical management and allows accurate identification of the relatives who are at risk [10, 11].

So far more than a 100 aneurysm gene association studies have been reported involving many connective tissue, signaling pathways, cardiovascular and immune genes as possibly associated to aneurysms. However, some of the finding from these studies have failed to be replicated in a different sample set or the size of the study was not large enough [11]. The most commonly used methods for investigating the relation of genes with aneurysms are through single nucleotide polymorphisms and family based DNA studies [10, 11]. Studies which investigate the gene expressions from aneurysmal and healthy aortic tissue reveal the differences only at the end stages of the disease where the vessel wall architecture has significantly been altered [4]. An alternative method for studying the disease at its developing stage is the use of knock out mouse studies, here a candidate gene is deleted from the mouse in order to observe its effect on the animal. However, this approach is very time consuming, expensive and attracts ethically concerning. Despite their contribution, there are significant differences in disease progression and response to therapy between human and animal trials [11]. The underlying mechanisms leading up to the aneurysm formation aren't always the same in different species. Additionally, animal models can not represent the large selection of genetic variants possibly linked to AAA, present in human patients [11]. Studies designed to understand the structural and mechanical properties of the aneurysmal tissue often use human samples extracted during open vascular repair operations and it is only representative of the end stages of the disease [4]. While these studies help understand the consequences of aneurysm on the vessel wall, it isn't possible to study the underlying mechanisms leading up to the aneurysm formation using the extracted tissue.

A genetic variant can be described as a change in the DNA nucleotide sequence. This alteration can be benign, pathogenic or of unknown significance. Benign variants have no functional effect on the gene product while pathogenic variants may disrupt the functionality. Variants of unknown significant are classified as such since enough data has not been collected on their effect yet. A variation in the DNA sequence may result in a nonsense (null), missense or a silent mutation. A null mutation causes the amino acid chain that is coded by the original gene to terminate prematurely, resulting in a shorter polypeptide chain or a lower quantity of this protein. Whereas in a missense mutation,

a different amino acid replaces the original one, leading to a possible change or loss of function. In only a small proportion of aneurysm patients, a (likely) pathogenic variant has been identified, using the current stringent diagnostic molecular criteria. However, variants of unknown clinical significance in aneurysm genes occur at a much higher frequency [12]. Very often these variants are classified a such, because they are rare, and have not been reported before. To determine the effect of these variants in aneurysm genes, functional assays which display a change in the function of that gene product or dysregulation of the molecular pathways to which the gene belongs to, are needed to be established. For the aneurysm genes, which have an effect on structural integrity of the aortic wall, there are very few functional assays. Currently, there are no functional assays to establish if variants in collagen genes have an effect on ECM functionality. Here, there becomes a need for an alternative method for testing the subsequent effect of a genetic variant on the functionality of the relevant tissue or organ.
In the ongoing aneurysm study at the Departments of Clinical Genetics and Vascular Surgery at Erasmus MC, whole exome data is available from around 850 aneurysm patients from 650 families. This is the largest study to date. Pathogenic variants in *COL3A1*, one of the most abundant forms of collagen in arterial wall were identified in 8 families, so far. In around 100 families, a variant of unknown significance in one of the four aneurysm collagen genes *(COL3A1, COL1A1 – and A2 and COL5A1)* was observed. The importance of developing a method to establish the effects of these variants is becoming more clear since this is a potential way to distinguish between 1) benign variants that are not associated with extreme vascular and tissue fragility and 2) the variants that cause dysfunctional ECM remodeling because of insufficient or defective protein synthesis. This potentially may have a large impact on screening strategies and clinical management.

1.3. Tissue engineering for vascular disease models

Tissue engineering, in recent years, has become an alternative approach to animal models in developing tissue repair/replacement grafts or disease models [5]. There are several methods aimed at developing tissue engineered vascular constructs for studying human diseases; from scaffold based constructs to bioprinting and self-assembly approaches [13–15]. There are advantages and limitations for all of these methods. However, self-assembly and cell derived matrices have shown to have several advantages over scaffold based methods in mimicking native tissue and showing greater mechanical properties [15, 16]. The self-assembly methods were found to show a higher gene expression compared to monolayer cultures [17]. A disadvantage of using a cell-laden scaffold is that it is often difficult to attribute the observed properties to the scaffold biomaterial or to the contribution of the seeded cells [15, 16]. It is not possible to mimic the hierarchical architecture of an in vivo ECM using the currently available biomaterials. However, self-assembly could be a possible alternate approach where cells are seeded in high density and allowed to synthesize their own ECM. A study by Ahlfors et al. compares the mechanical and structural properties of tissue engineered constructs using, self-assembly and cell-seeded gel scaffolds. The results show the self-assembled constructs perform more similarly to native tissue in biomechanical tests [15, 16]. Additionally, a cell-derived

self-assembly approach allows observation of the native ECM produced by the cells as opposed to a pre-defined scaffold matrix structure [5]. This could potentially allow to observe any changes to the ECM products produced by cells collected from patients or the effects of certain treatments. One disadvantage of these self-assembly approaches is that often, an initial high density of cells and a long culture period is required in order to obtain robust constructs.

1.4. Motivation

For this study, in order to develop cell derived tissue engineered construct using patient cells, the self-assembly 3D ring culture system previously developed by Gwyther et al., using smooth muscle cells (SMCs), was chosen [13]. This system allows formation of small sized rings from human cells with the capabilities of producing their own ECM. It requires a short culture period with a high initial cell seeding density [13]. These rings can potentially be used for mechanical and structural characterization. The ring shape makes it easier to handle the constructs while mimicking a vascular geometry. This system can potentially be adapted for other types of cells and used to observe any mechanical or structural differences between the rings produced by healthy and diseased cells. Instead of using SMCs as done in Gwyther et al. and other studies which use the mentioned method, fibroblasts collected from AAA patients by skin biopsies were chosen. Similar to the SMCs fibroblasts are crucial in ECM remodeling, they produce high amounts of collagen and elastin and are a part of signaling pathways responsible from ECM maintaining homeostasis. Additionally, since they can be collected from patients via skin biopsies, as opposed to SMCs, access to this type of patient cells is easier. This approach could be developed as a potential functional assay allowing to identify the effects of a genetic variant likely associated with AAA. It may test the ability of self-assembly into a 3D construct and identify mechanical or structural differences in the ECM they produce. For this study 3 patients with AAA, who have different pathogenic genetic variants in aneurysm genes were chosen. The patients P1, P2 and P3 have *COL3A1* null, *COL3A1* missense and *TGFBR2* mutations respectively. Two lines of age and gender matched cells were used as controls. The chosen patients all have genetic variants in aneurysm genes that are known to be pathogenic which allows to validate whether this approach may be used to observe their functional effects.

1.5. Aims of the Study

The motivation behind this study was to develop an in-vitro model of a vessel wall using patient cells to study its morphology and mechanical properties in relation to the functional effects of the specific genetic variants present in the patients. As an initial step towards the development of this model we aimed to design a work flow allowing patient cell derived tissue rings to be produced and characterized.
The aims of this study were defined as the following:

1. Design and Fabrication of the cell culture mold system for producing scaffold free, 3D, cell derived tissue rings and the adjustment of the suitable mechanical testing setup
2. Adjustment of the culture conditions for the use of fibroblast cells obtained from patient biopsies to produce fibroblast tissue rings.
3. Structural and mechanical characterization of the fibroblast rings through histological staining and studying the ring development process through time- lapse images.

1.6. Study outline

The study was carried out in two stages as described below:

1. The culture molds and the test setup were fabricated and adjusted for the formation and the characterization of tissue engineered rings.
2. The culture conditions were optimized and the produced rings from patient and control rings were characterized in terms of overall morphology, ring thickness and collagen production using histological stainings and the ring formation stage was observed using time-lapse images.

2

Materials and Methods

2.1. Design and Fabrication of the Ring Culture System

2.1.1. Mold Design and 3D printing

In order to culture the cells in a 3D, scaffold free manner that is suitable for mechanical testing, the tissue ring self-assembly method designed by Gwyther et al. and modified by Strobel et al. was chosen [13, 18]. The agarose molds for cell seeding were fabricated as previously described in Strobel et al. [18]. The final mold was achieved in 3 steps; an initial 3D printed mold, an intermediary negative PDMS template and a final agarose mold which the cells were seeded in.

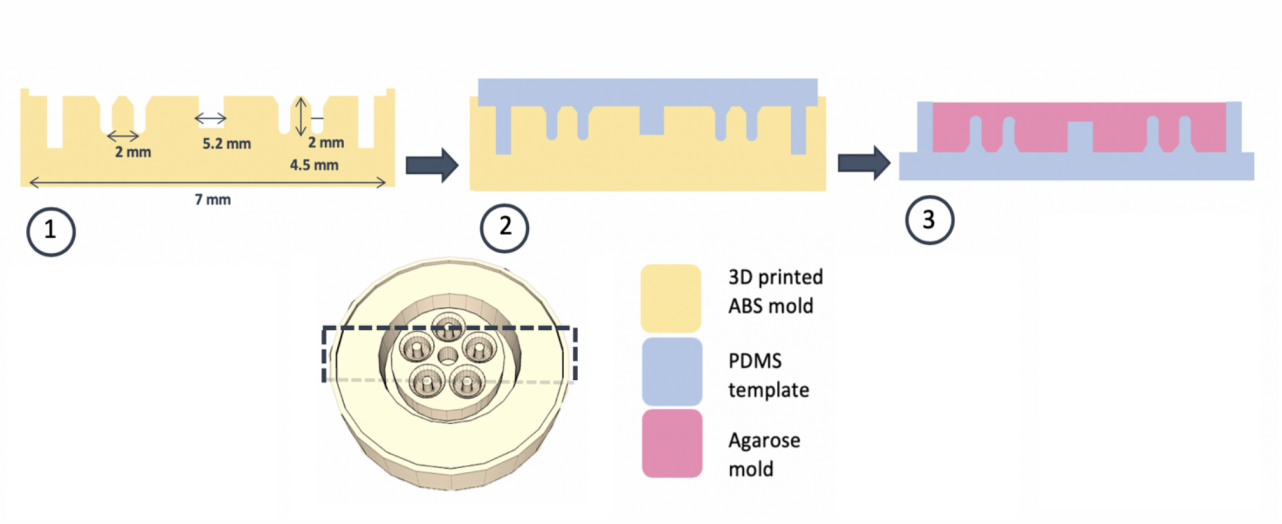

Figure 2.1: Mold Fabrication Process. Step 1 shows a cross-section of the 3D printed mold with the specific dimensions. In step 2, PDMS (shown in blue) was cast over the printed mold. After PDMS was fully cured it was removed from the mold and sterilized. In step 3, 2% agarose dissolved in DMEM was poured into the PDMS template to obtain the final mold.

First a CAD (Computer Aided Design) model for the 3D printed mold was designed using SketchUp (Trimble) software, according to the dimensions presented in Figure 2.1. Briefly, the mold was circular, containing 5 annular wells. The inner post diameter of each well was 2 mm, with a surrounding well diameter of 6 mm. The 45° tapered edges around the opening of the wells were designed to allow easier pipetting and removal of the rings. The 2 mm diameter post was chosen in order to produce rings using a relatively low number of cells compared to 4 mm or 8 mm that are used in the study. A single mold was designed to fit inside one well (34.8 mm in diameter) of a 6-well cell culture plate. After the design was completed the STL file of the CAD model was converted to a G-code file using the slicing application Ultimaker Cura 4.0 (Ultimaker). The slicing application cuts the model from the STL file into thin sections allowing the 3D Printer to print the model, layer by layer, following this file. The CAD model for the 3D printed mold is shown in Figure 2.2 (A), an X-Ray cut of one of the cell seeding wells can be seen in B. The same model is then uploaded to a slicing software, here the printing pattern that the printer nozzle will follow is shown in green (C). The printer nozzle diameter was 0.25 mm and the infill parameter was chosen as 30%, which describes how dense the printing pattern will be for each layer, it is possible to obtain a strong enough structure while preserving material by choosing an optimum infill density. After the printing settings were chosen and saved to the SD-card of the printer, the model was 3D printed via an Ultimaker 2+ (Makerbot) 3D printer using Acrylonitrile butadiene styrene (ABS) as the mold material. It was important that the mold material could endure 60°C of heat and provided a smooth finish for the following steps. The smooth finish is required to obtain a smooth final mold in which the cells' behavior is not influenced by any ridges or surface obstacles.

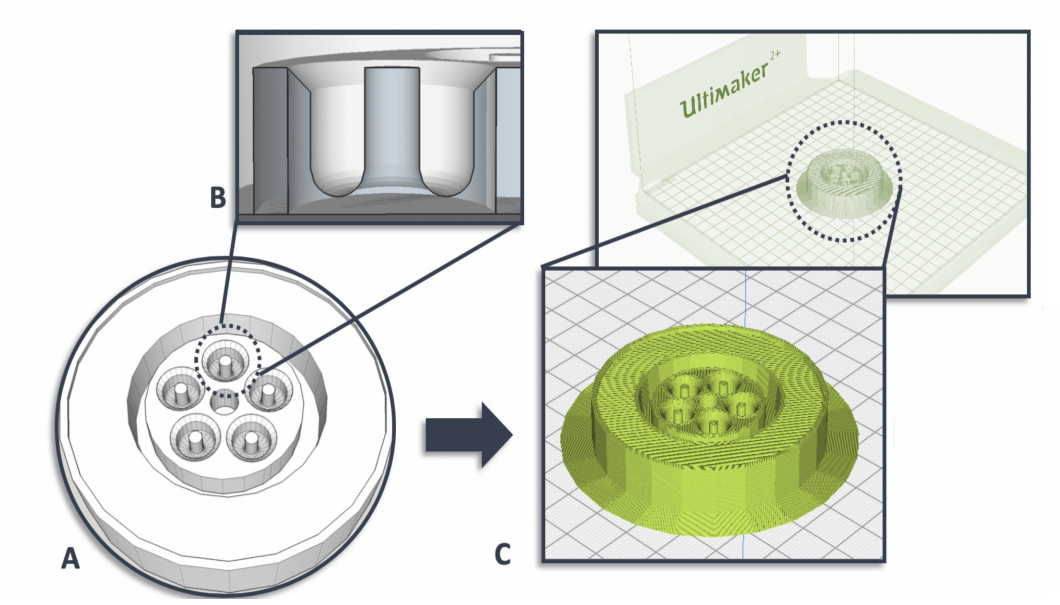

Figure 2.2: A) The mold model designed in SketchUp CAD software, this model was designed according to the dimensions provided in Strobel et al. [18]. B) Figure shows a side-view of an X-Ray cut of one of the wells inside the mold, showing the central post and the well around it. C) The model in Ultimaker Cura, sliced in thin layers for printing. The path which the printer head will follow to print the model can be seen.

2.1.2. PDMS Intermediary Template

The next step was to obtain a negative template of this mold, which functions as an intermediary template before the final agarose mold. For this, Polydimethylsiloxane (PDMS; Sylgard 184, Dow Corning, Midland, MI) was cast over the ABS mold. PDMS consists of 2 components, the curing agent (cross-linker) and the base component, as shown in Figure 2.3(B). These were used in a 1:10 (w/w) ratio, by weighing the components on a scale and mixing in a plastic cup. PDMS was thoroughly stirred using a spatula for 2-3 minutes. This process generated air bubbles which were then degassed using a vacuum desiccator for an hour. The ABS mold was covered with a wall of tape around the edges, as shown in Figure 2.3, in order to avoid any leakage of PDMS during degassing or curing. After making sure there were no air bubbles left, the mixture was carefully poured over the ABS mold and placed in the desiccator for another hour to eliminate any new air bubbles. After getting rid of the air bubbles the mold with PDMS was left to cure in an oven at 60°C for at least 4 hours.

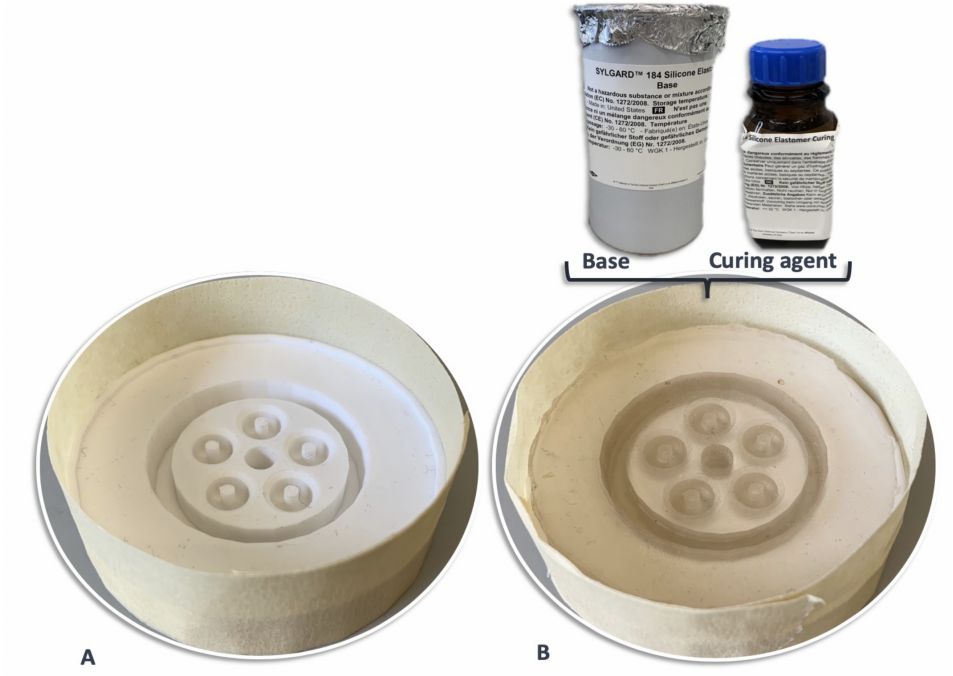

Figure 2.3: A) ABS mold with a tape wall around the edges. During degassing the air bubbles inside the PDMS begin to move to the surface causing the mixture to rise, the tape helps avoid leakage and allows room for a thicker bottom for the PDMS template. B) The ABS mold with the cured PDMS inside ready to be peeled off.

2.1.3. Final Agarose Mold

Agarose is a commonly used material in biological applications due to its biocompatibility and non-adhesiveness [8]. Since the cells can not adhere to the mold surface, they attach to each other and it is possible to remove the rings after the appropriate culture period. To prepare the final mold, first 2% Agarose (Sigma-Aldrich) was dissolved in Dulbecco's Modified Eagle Medium (DMEM; Sigma-

Aldrich), by heating the mixture in a microwave for 1-2 minutes, making sure it is fully dissolved. The solution was kept in a 4°C fridge until used for mold making. The agarose molds were prepared one day before cell seeding. The dissolved agarose, PDMS molds and any other tools, like tweezers for removing the mold from the template, were autoclaved in order to maintain sterility. Since agarose solidifies at room temperature, it was important to maintain the solution in a heated water-bath while making the molds. Following the autoclave process, 4ml of agarose was pipetted in the PDMS template surrounding the wells without filling the actual wells. In order to prevent any air bubbles inside the agarose mold, especially inside the posts, 1 ml of agarose was pipetted inside each well individually, as shown in Figure 2.4.

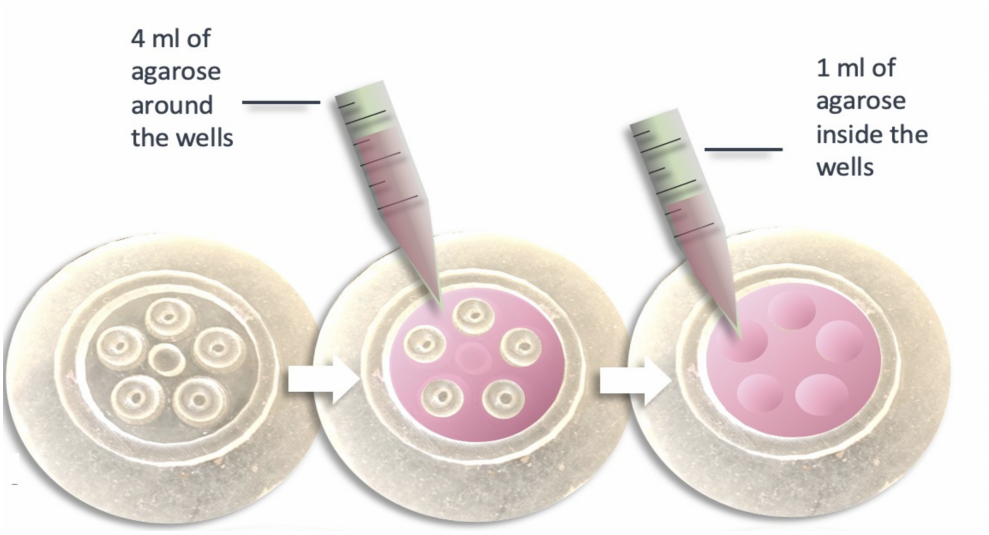

Figure 2.4: The process of making the agarose mold. 4ml of agarose solution was pipetted inside the PDMS template, first by leaving out the wells and later filling the insides of the wells with 1 ml of agarose solution. This made sure the wells were all filled with agarose and no air bubbles were trapped, preventing the central post formation in the final agarose mold.

2.1.4. Custom designed hooks for the mechanical test setup

For mechanical testing, a previously designed in-house uniaxial tensile tester was modified for ring testing. The system briefly consisted of a linear actuator [Oriental Motor Ltd., Tokyo, Japan], a 0.5N load cell (Omega Engineering, Inc., Norwalk, CT, USA), a digital multimeter [Siglent (SDM3045X) Technologies Co., Ltd., Shenzhen, China], a stationary clamp attached to the load cell and a moving one connected to the actuator and finally a water-bath for maintaining the samples warm and humid. The stretch of the samples was recorded using a digital microscope camera [Carl Zeiss Microscopy GMBH, Jena, Germany] and the lighting was adjusted using two small light sources connected to the system.

In order to adjust the setup for testing the rings, first, suitable grips were designed as two steel pins with a diameter of 1 mm, attachable to the existing clamps, as shown in Figure 2.5. The pins were overhung the water-bath so that they were submerged in Phosphate Buffer Saline (PBS) (Lonza), making it easier for the rings to be placed through the pins using thin rounded forceps. In order to

mount the rings on the system, the two pins were brought close enough so that they were touching, with the aid of thin rounded forceps the rings were lifted from the PBS containing dish and carefully threaded over the pins which were submerged in PBS.

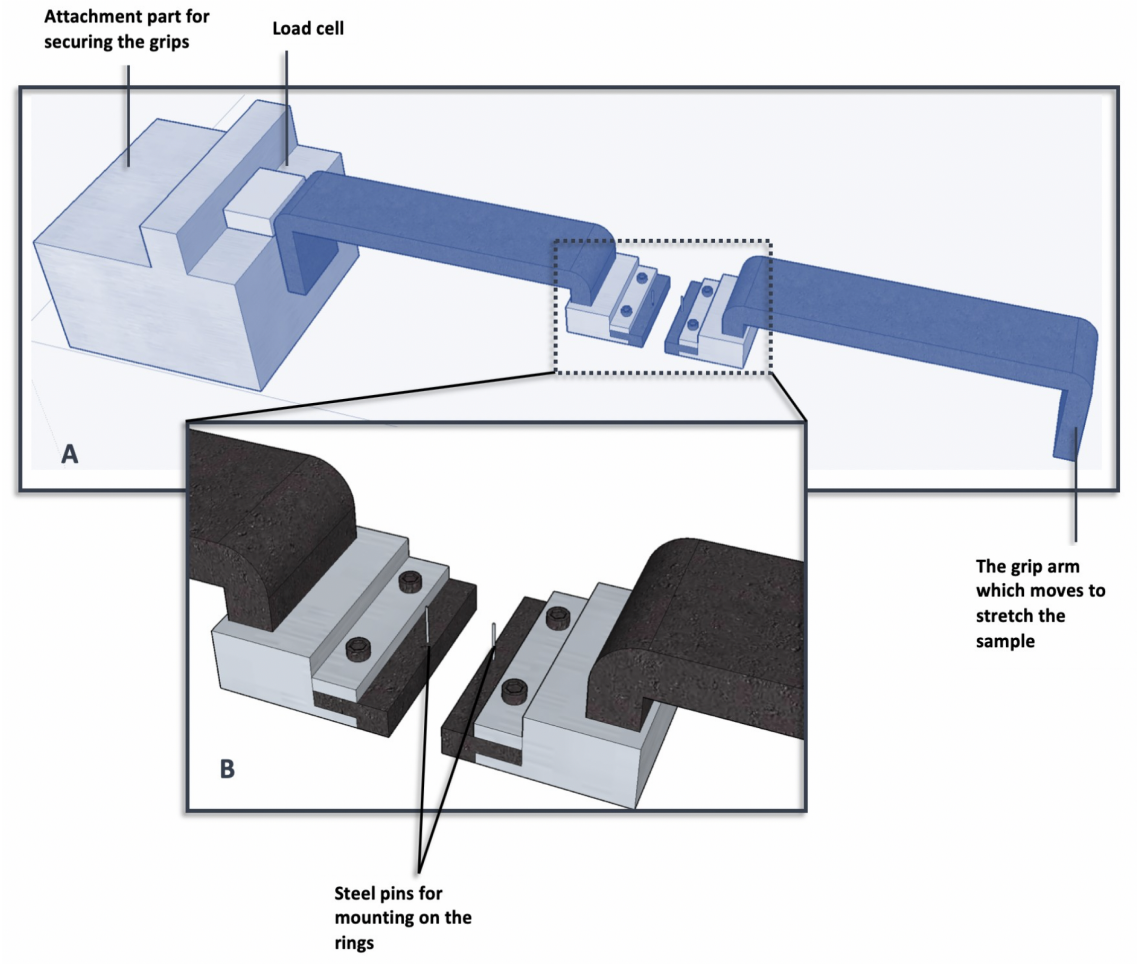

Figure 2.5: A) The grips, consisting of two lever arms and steel pins on the ends to thread the rings through, were custom designed to be suitable for the previously built in-house tensile test setup. B) A close-up of the grips showing the pins, the diameter of the pins are 1 mm each. The lever arms overhangs the water-bath, so that the pins are submerged in PBS during testing.

2.2. Self-Assembled Ring Formation and Characterization

2.2.1. Cell Culture

Fibroblasts obtained from the skin biopsies of AAA patients were isolated and expanded in DMEM (Sigma-Aldrich) supplemented with 10% FBS (Sigma-Aldrich) and 1% penicillin/streptomyocin (Sigma-Aldrich) in T75 flasks. 3 different patient cell lines (P1, P2, P3) and 2 different control lines were used. Age matched healthy fibroblast cells were similarly cultured in the culture media as control cell lines. Cells of passages 5-8 were used. Cells were maintained at 37°C in a 5% CO2 incubator.

Culture media was refreshed twice a week and when the cells were 90% confluent they were passaged to new flasks using 1.5 ml of trypsin-EDTA(Sigma-Aldrich). Confluency defines, how much of the flask is covered by the cells, once the cells reach a certain confluency they no longer proliferate and begin to die, at this stage they should be passaged to new flasks in a lower concentration until they grow again. In order to passage the cells, when they were 90% confluent the cells were washed with 10 ml of 1X PBS and trypsinized with 1.5ml of trypsin-EDTA, to detach the fibroblasts from the bottom of the flasks. They were incubated for 5 minutes at 37°C and resuspended in 8.5ml of culture media. The cell suspension was divided between two new flasks and additional fresh culture media was pipetted in each flask to maintain all the cells in 10ml of culture media. Since a large number of cells were required for the rings, sub-culture of the fibroblasts in T75s were continued until there were 3-4 flasks from each.

2.2.2. Cell Seeding

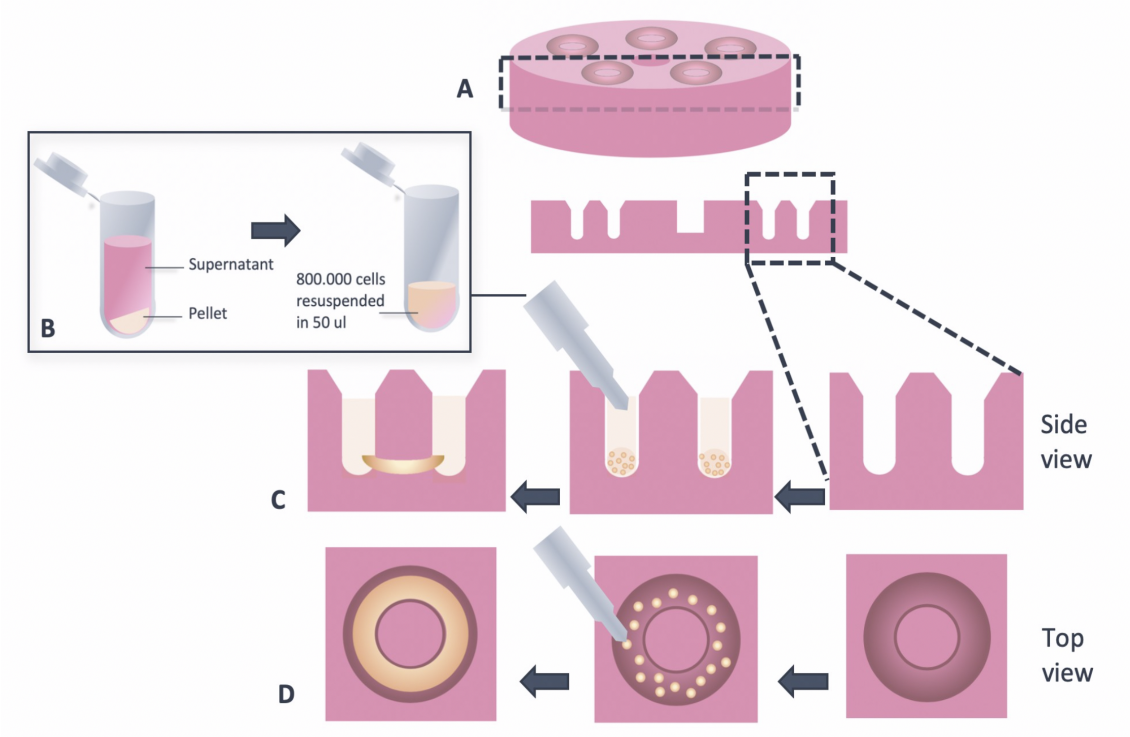

Figure 2.6: Cell Seeding Process. A) Agarose mold and its cross-section. B) Fibroblasts were resuspended in high appropriate concentration after centrifuging to obtain the required cell concentration for forming rings. C) The side view of the cell seeding and ring formation processes into one of the wells. D) The same process shown from the top view. The 50µl of cells suspension with 800.000 fibroblasts is seeded into each well. In 48 hours the cells contracted around the post to form a ring.

Figure 2.6 above shows the process of cell seeding into the agarose wells. Once the fibroblast cells were 90% confluent, they were trypsinized and detached from the flasks. Cells were counted using trypan blue dye (Lonza) and an Automated Cell Counter (Bio-Rad). 10µl of the cell suspension and

10µl of the trypan blue dye were pipetted in a vial and mixed. 10µl of this solution was loaded in a cell counting slide and the slide was inserted in the Automated Cell Counter. In order to prepare at least 5 rings per each cell type, the appropriate amount of cell suspension was pipetted out into a falcon tube from the entire cell stock and centrifuged for 5 minutes at 1000 rpm. As shown in Figure 2.6 (B), the supernatant culture media was aspirated out and the remaining pellet of cells were re-suspended in the appropriate amount of culture media depending on the number of desired rings. 50µl of cell suspension was then pipetted into each well.
After all the wells were seeded with cells, 2 ml of culture media was poured in to the 6-well plate surrounding each agarose mold without fully submerging the molds. The 6-well plate was then kept in a level incubator at 37°C in 5% CO2 and left undisturbed for 48 hours. After 48 hours, culture media was replaced with 4 ml of fresh culture media, fully submerging the molds. The culture media was refreshed every other day and rings were cultured for 8 days.
In order to determine the optimum cell seeding concentration, rings using healthy control fibroblasts were prepared in two different concentrations. First they were prepared using 500.000 cells per ring and later as 800.000 cells per ring.
To observe the ring formation via cell aggregation, one separate mold was prepared for recording time-lapse images of the process by the CytoSMART system (Lonza).

2.2.3. Time-lapse Images

Immediately after the rings were seeded, one mold was placed under the CytoSMART imaging system in order to record the ring formation by self-assembly process. The system allowed for imaging a quarter of a single ring at a time as can be seen in Figure 2.7. The mold was not moved for imaging the rest of the ring, in order to prevent the motion from interfering with the ring formation process. Initially the time-lapse images of control cells seeded in two different cell densities were taken every 5 minutes for the period of 8 days in order to determine the effect of cell density on the kinetics of self-assembly. Following this, time-lapse images of each cell line (controls and patients) were taken over a period of 2 days to observe the effect of the patient cases. The time cells need to form a stable ring was determined by these images. The ring contraction due to the cell aggregation was measured using the change in the area the initially seeded cells occupy inside the culture wells by ImageJ software.

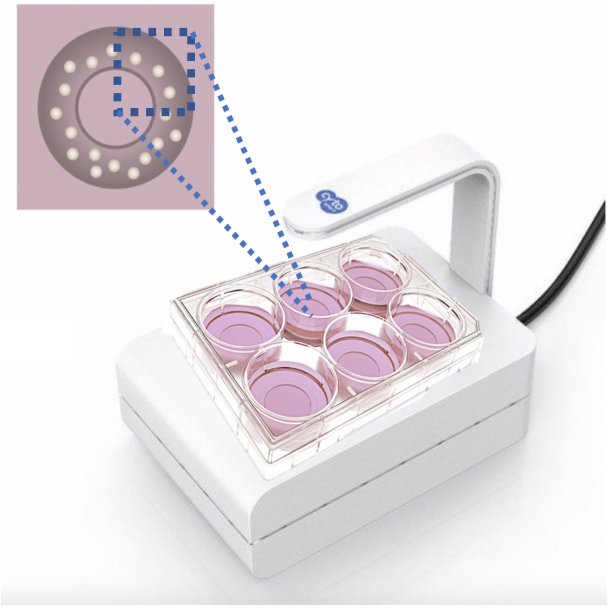

Figure 2.7: A representative schematic showing the CytoSMART system, It is possible to track cell aggregation which results in the ring formation by taking periodic images of a quarter of the ring.

2.2.4. Histology

In order to observe the rings structurally on a microscopic scale, the cultured rings were prepared for histology. Rings cultured for 8 days were carefully removed from the molds, using thin rounded forceps. The central post was cut from the top in order to allow room for the forceps. With the aid of the forceps the rings were gently pushed upwards and removed. The rings were then washed in PBS. Next, they were placed inside embedding biopsy cassettes in separate compartments for each ring.

The samples inside the cassettes were then fixed in 4% paraformaldehyde (PFA). Fixation allows the structure to remain intact without degenerating until staining and imaging stages. The fixed samples were left in the PFA for at least a day in room temperature and then embedded in paraffin following dehydration in a graded ethanol series and clearing in xylene.

The paraffin blocks were later sectioned into 5µm thin sections using a manual microtome. First the paraffin block were placed to cool on an ice tray, which allowed a more uniform and a smooth section to be sliced. The block was then secured on the microtome and cut into sections of 5µm. The cut slices were placed on a warm water bath to stretch and carefully separated from each other with the aid of a sharp knife. The individual sections were then adhered on the Superfrost Plus slides. Following this the slides were left to dry in an incubator overnight at 37°C.

For visualizing the general structure of the rings and specifically the collagen produced by the fibroblasts, slides from each cell line were stained with hematoxylin and eosin (H&E), and Picrosirius Red (PSR). The H&E is used to stain the cell nuclei dark purple and the cytoplasm pink allowing to observe the overall tissue structure. Picrosirius Red staining is specific to collagen and stains collagen fibers red.

The slides were imaged using Nanozoomer scanner [Hamamatsu, Japan], allowing high resolution images. The scanned images were analyzed on the NDP.view2 software [Hamamatsu, Japan]. The quantification of the amount of collagen fibers in the rings were conducted using the image analysis software, ImageJ, via thresholding and calculating the percent area fraction of red stained areas. Additionally ring thicknesses, distribution of cells and collagen fibers within the rings were also analyzed using the histology images and ImageJ.

2.2.5. Mechanical Test

The mechanical testing of the tissue rings were planned to be conducted using a previously mentioned, in-house tensile testing machine adjusted for ring testing. The setup is briefly shown in Figure 3.2. A load cell of 2.5N was used (A). The lever arms were brought together so that the steel pins were touching. The control rings were gently threaded through the steel pins, using thin forceps, making sure they were submerged in PBS. The parameters for testing were adapted from Gwyther et al., a tare load of 5mN was applied and the gauge length was recorded [13]. The rings were preconditioned for 5 cycles. Preconditioning is applied to obtain repeatable mechanical results. Following the preconditioning cycle the rings were stretched until failure with a strain rate of 10mm/min. The force and displacement was recorded throughout the test, the displacement was measured as the distance between the two pins. Prior to the mechanical testing the rings were removed from the molds and maintained in a petri dish containing PBS. The ring thickness were recorded using a digital caliper from at least three different points on the ring. This thickness was used to calculate the cross-section area of the rings where a circular cross-section was assumed. The mechanical testing was conducted using rings from control cell lines (n=5), however it was not possible to obtain meaningful results using the current setup and the patient lines were not robust enough for a mechanical test. Therefore the mechanical tests were not included in the characterization of tissue rings prepared in this study.

2.2.6. Statistics

Two batches of rings were prepared for the time-lapse images; 2 sets of rings from each cell line (2 control and 3 patient lines) were measured for the calculation of the ring contraction. The data for the final mean thicknesses calculated using the histology images were reported as mean thickness ± standard deviation. The thickness values are reported as overall patient ring thickness (n = 6) and the thicknesses of individual patients rings with specific genetic variants (n=2 from each patient). The same batch of rings were used to calculate the % area fraction of collagen. A one-way ANOVA test was conducted to show the significant differences between overall patient and control groups for final thickness and % area fraction of collagen. This was not performed for each individual patient lines due to the low number of samples.

3

Results

In this chapter the results of the two sections, 1) the design and fabrication of the scaffold free 3D culture system and 2) the ring formation and characterization are presented. The fabrication of the ring culture molds consisted of three intermediary stages. In addition to the culture mold, the in-house tensile testing device was modified to be suitable for the testing of the cell aggregated rings. In the ring formation and characterization section, the process of how the rings form, their final thickness and the production of collagen by different cell lines are presented. The table below gives an overview of the planned experiments for the characterization of the cell aggregated rings however as can be seen from the table, some of these experiments could not be conducted due to a persistent contamination at the sub-culture stage of the fibroblast cells, which was the main material of the experiments. The contamination caused a failure to produce enough number of samples and repeats of the previously conducted tests and prevented further experiments being conducted in time. However, from the results presented in the further sections, it is possible to observe the kinetics of cell aggregation for ring formation, effects of cell seeding density, ring thickness and production of cell derived collagen by both patient and control cell lines.

Experiments for Ring Formation and Characterization	***Conducted/Failed***
Optimizing cell seeding density	Successfully conducted using control cell lines
Optimizing culture media refreshment time	Successfully conducted using control cell lines
Mechanical test (controls only)	Mechanical test setup required a more sensitive load cell to record relevant forces. A more sensitive load cell was ordered.
Cytomate (all cell lines)	Successful for all cell lines
Histology (all cell lines)	Successful for all cell lines
Mechanical test (all cell lines)	Couldn't be conducted due to contamination. Patient cells were too fragile to be mounted on the test setup.

3.1. Design and Fabrication of the Ring Culture and Mechanical Testing Setup

This section presents the results of the each step from the culture mold fabrication process and the adjustments made to the mechanical test setup.

3.1.1. Fabrication of the ring culture molds

The final ring culture mold was successfully prepared in three steps; an initial 3D printed mold, a PDMS intermediary template and a final agarose mold. When the 3D print was completed the mold was washed with water and detergent making sure there are no residues left inside. A single 3D ABS printed mold was used for preparing 3 PDMS templates, the ABS mold was able to endure multiple cycles of heating for the production of the PDMS template. It was possible to make sure the PDMS has cured by checking the surface for any tackiness. Once the PDMS had completely cured it was carefully peeled off from the ABS mold. Since PDMS is an autoclavable material, it was possible to use the templates multiple times to make more agarose molds. 3 PDMS templates were prepared in order to simultaneously create multiple agarose molds before the agarose solution solidifies at room temperature. It was important to make sure the agarose solidified with a flat surface. In order to successfully remove the agarose molds from the PDMS templates, without breaking the central posts, the agarose solution was left to solidify for at least 6-7 minutes and was removed carefully using tweezers. The final agarose molds were then placed in a 6-well plate. They were fully submerged in 4.5 ml of culture media and left in the incubator overnight in order to equilibrate. The agarose molds were prepared a day before cell seeding to let them equilibrate in the culture media overnight. Each mold was used only for a single cell line. The products of each step are presented in the Figure 3.1 below.

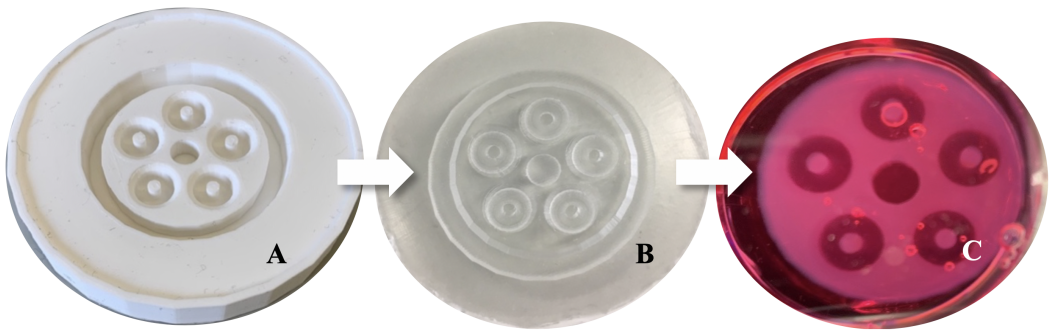

Figure 3.1: A) The 3D printed mold B) Intermediary PDMS template, 3 of these were prepared. C) The final agarose mold submerged in culture medium inside a 6-well plate.

3.1.2. Fabrication of the custom hooks for mechanical testing

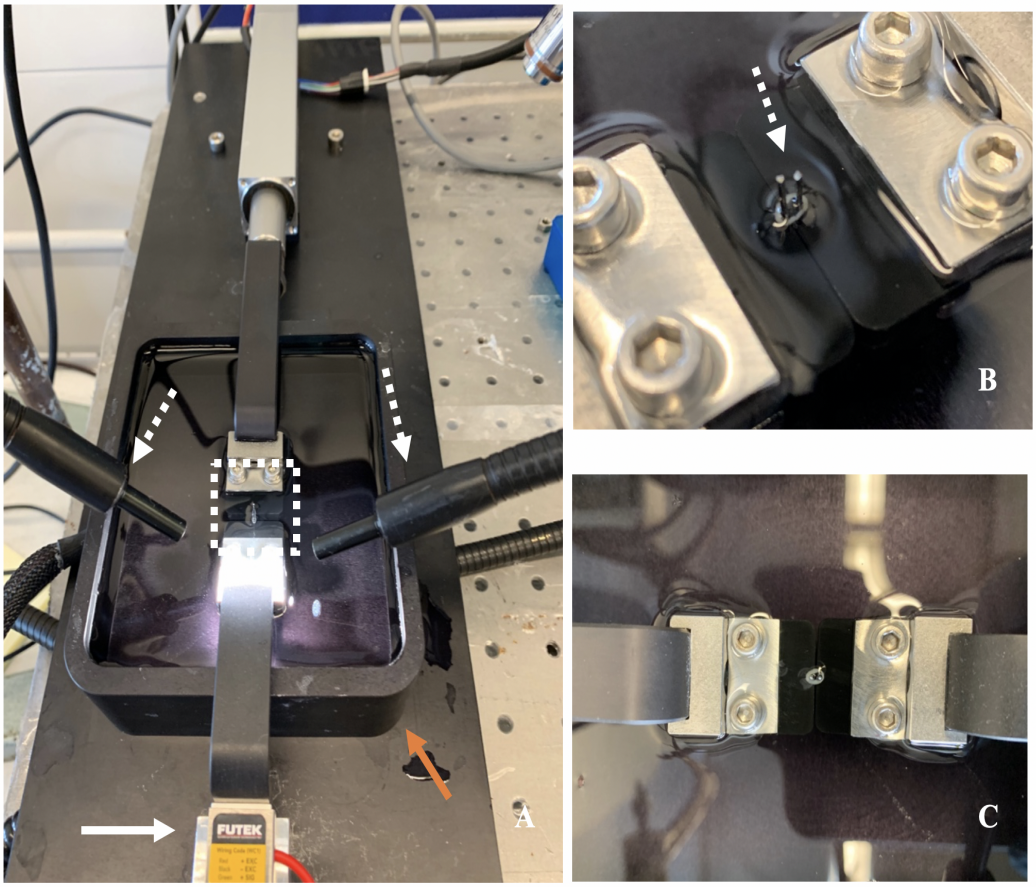

Figure 3.2: A) The overall mechanical test setup. The white arrow indicates the load cell, dotted arrows show the light sources for illuminating the sample for a better recording and the orange arrow points to the water-bath in which the samples would be suspended in during testing. The selected region indicating the steel pins used as hooks for samples to be mounted on is magnified in B.

The fabricated lever arm which can be attached to the in-house tensile testing device are shown in Figure 3.2, indicated with dotted white arrows. One of the lever arms connected to the pin was stationary while the other was connected to an actuator causing the samples to stretch during testing. At the ends of the lever arms which were submerged in the water-bath containing PBS were two steel pins of 1mm diameter each. These pins were brought together to thread the tissue rings through as seen in Figure 3.2 (B).

3.2. Fibroblast Aggregated Ring Tissue Formation

The optimization of the cell seeding conditions were conducted using the control cell lines. Within 24 hours after the initial cell seeding, it was possible to see an opaque white ring form around the central post as shown in Figure 3.3. All of the rings which were seeded initially formed a ring, any

breakages or non-uniformities developed at later stages during the culture period. Since the agarose mold was non-adhesive to the normally adherent fibroblast type cells, the cells were initially found in their circular detached morphology, covering the bottom of the cell culture well, shown in Figure 3.3 (C). The initially spread out detached cells, attached to the neighboring cells instead and contracted to form a cell aggregated tissue ring. The rings had clearly contracted around the central post and detached from the rest of the mold as shown in Figure 3.3 (B), in the close up image of a single ring. An overview of the self-assembly of the rings into a ring is shown in Figure 3.3 (C-E). These images were taken immediately following cell seeding (C), 12 hours (D) and 24 hours after (E). The number of rings which were successfully cultured based on different conditions are presented in Table 3.1.

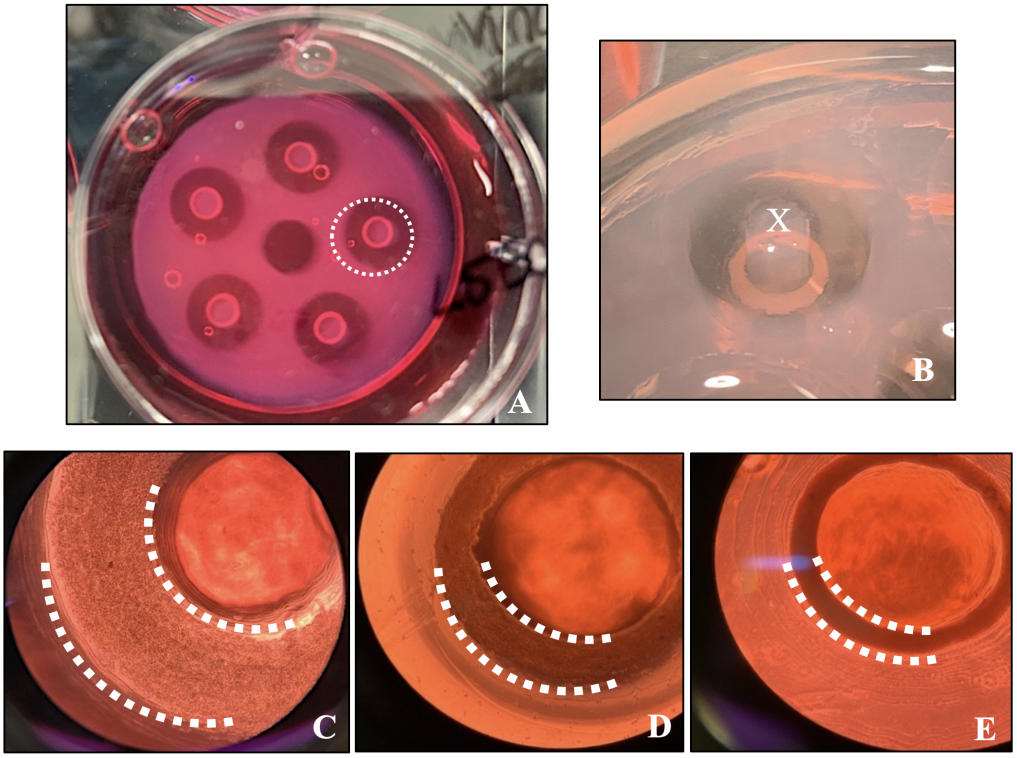

Figure 3.3: A) An agarose mold from the top view, with 5 successfully formed fibroblast rings which appear as white rings around the central posts, 24 hours after cell seeding. B) A close up image of a single ring from the side view, the top of the central post is marked as x and the fibroblast ring can be seen as the white tissue contracted around the post. Figures C, D and E show a close up of the rings inside the molds from the top view, the change in ring thickness due to cell aggregation and contraction around the post can be seen over the course of 36 hours (scalebar = 2 mm). C) Immediately after cell seeding, the individual cells can be seen as their detached circular form spanning the bottom of the well. B) 24 hours after cell seeding the cells have aggregated and attached to each other to form a ring around the central post, at this point it is possible to observe a ring as shown in B. E) 48 hours later the ring has contracted even further forming a more robust ring.

3.2.1. Cell Seeding Conditions

Initially, the cells were seeded and left undisturbed without a culture media refreshment for the first 24 hours. However this led to some rings breaking right after the wells were flooded with culture

media.

The time lapse images from the CytoSMART system showed that cell aggregation was still ongoing for the first 2 days, which may have been the reason for ring breakage when the cells were disturbed with culture media early on. Later, the optimum time point for changing the media was determined to be 48 hours without disturbing the ring formation. This led to fewer rings breaking as shown in Table 3.1.

Another parameter for optimizing the conditions for fibroblast rings was the cell seeding density. Two different cell seeding densities of 500.000 per ring and 800.000 per ring were used. While it was possible to obtain tissue rings using both densities, the higher cell density produced more consistent and thicker rings. Two batches of rings were seeded to obtain a total of 5 rings per batch, out of the 10 overall seeded rings, 4 broke when a lower cell density was used and the culture medium was replaced after 24 hours, while all of the seeded rings survived when they were seeded in a higher cell density and left undisturbed for 48 hours.

Table 3.1: The table shows the number of successfully formed rings based on the culture media change and cell seeding conditions. 10 rings were seeded using both conditions and the number of successful rings are presented below. Using a high cell density with leaving the cells undisturbed for at least 48 hours was determined to be the optimum conditions for obtaining successful and robust rings.

Cell Seeding Concentration	**Culture Media Refreshment Time**	**Number of Rings Formed**
500.000 cells per ring	24 hours after cell seeding	6/10
	48 hours after cell seeding	8/10
800.000 cells per ring	24 hours after cell seeding	9/10
	48 hours after cell seeding	10/10

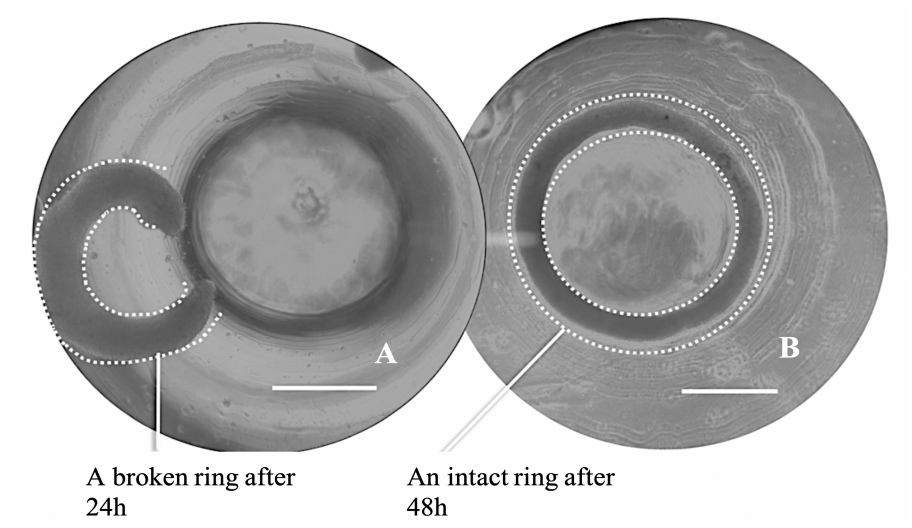

Figure 3.4: Microscopy images of two fibroblast rings after 24 hours and 48 hours. A) The ring which had appeared to form, was broken immediately after being flooded with culture media 24 hours after cell seeding. B) The ring from the same cell line had aggregated into a ring in the first 24 hours and left undisturbed for 48 hours, remained as a ring when flooded with culture media (scalebar = 1mm)

Figure 3.4 shows an example of how the initially formed rings break and contract when they

were prematurely flooded with culture media (A). The broken rings, which were separated from the central posts, initially maintained their ring like structure for a brief period of time and then contracted further, losing their shape. However the ones which remained without breaking when left undisturbed maintained their ring shape even after when they were removed from the molds at the end of the 8 day culture period, as can be seen in Figure 3.7 (G).

3.2.2. Kinetics of Ring Formation: optimization

Time lapse images acquired from the CytoSMART system were used to determine how the ring contraction changed over the course of 2 days and to observe the process of self-assembly.
The images showed the detached cells spanning the bottom of the wells initially lay flat and after some time began to cluster and climb on top of each other forming a more compact structure, the motion of the cells can be better understood via the time-lapse videos. These cells formed a ring like structure within the first 12-18 hours and then continue to contract into their final thickness following this. The phenomena can be described in two phases. In Figure 3.5, (through B-E), time-lapse images of ring formation is provided. Initially, it was possible to identify individual cells and observe how they move towards each other and attach (B). Once they have adhered to each other and formed a ring like structure it was still possible to observe the cells around the edges (C). These stages of self-assembly was complete within the first 12-18 hours. Following this stage, the ring structure contracted and gained an opaque look where it was no longer possible to distinguish the individual cells (D) This stage corresponded to the sharp decline in the ring thickness measured in Figure 3.5 for each cell seeding density (between 12-18 hours for high cell density and 18-24 hours for low).
The change in ring contraction slowed down after the second day, which was chosen as the time point for initial refreshing of the culture media without disturbing the ring formation. The speed of ring contraction for the two cell seeding densities is shown in Figure 3.5. The initial 12 hours for both cases showed a similar trend where the cells were assembling into a ring shape. The rings with a higher cell density formed a visible ring faster than the lower density condition. The contraction of the rings around the post plateaued after 18 hours for the high cell density ring and after 24 hours for the low cell density ring. This corresponded to the time when both cases have formed a ring such that the individually detached cells can no longer be distinguished. As can be seen from the Figure 3.5, after the cell aggregation into a ring form is completed, the ring thickness does not change throughout the culture period after these time-points. The difference in thicknesses of the two cell seeding conditions was maintained throughout the culture period. At the end of the culture period the rings were removed from the molds and their final thicknesses were measured using a digital caliper as 0.27 ± 0.10 mm (n=3) for the lower density and 0.58 ±0.15 mm (n=3) for the higher density rings. The discrepancy in these values with what is measured using the CytoSMART data is the due to the fact that the rings form a slightly tubular shape, their height along the central post (side view) is greater than their thickness measured from the top view.

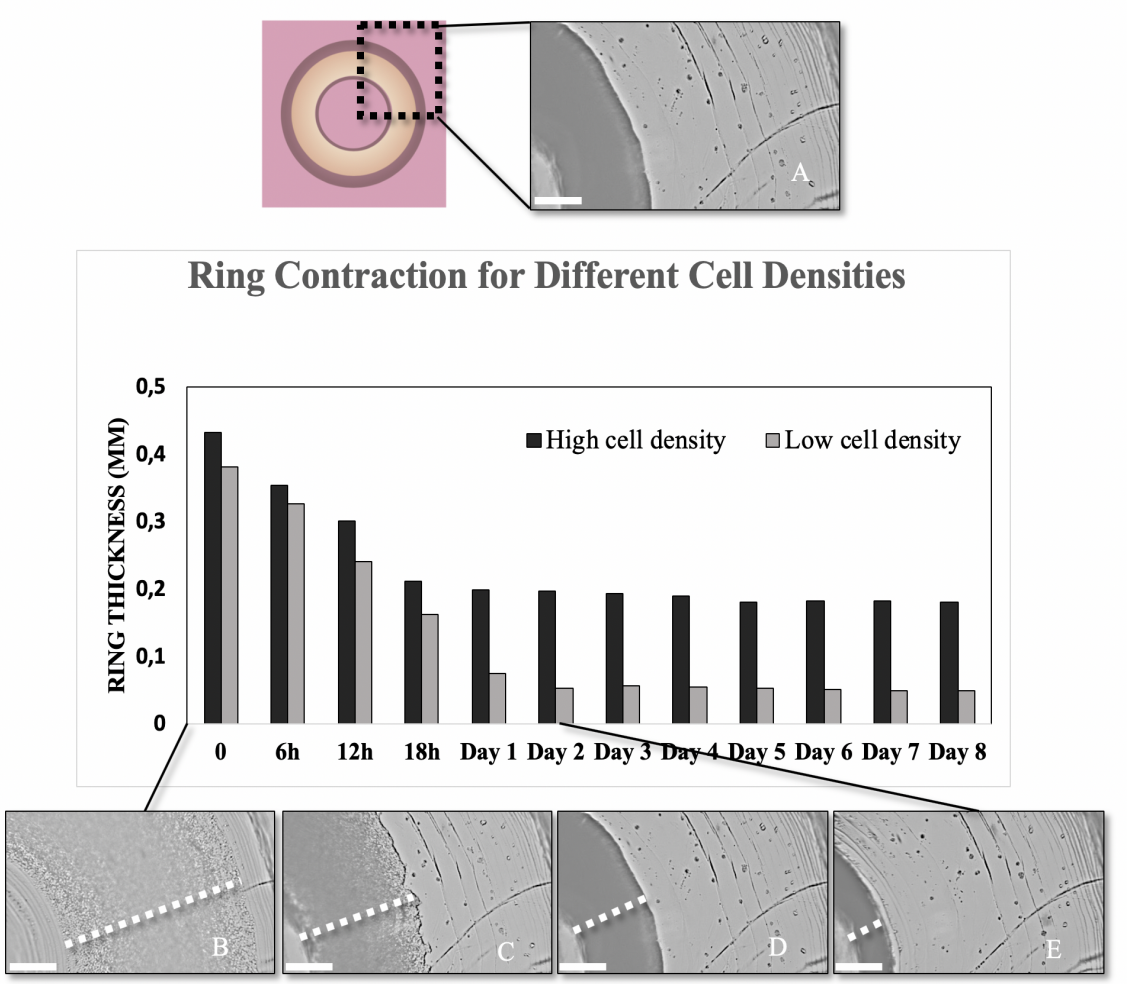

Figure 3.5: A) The CytoSMART system allows for imaging only a quarter of the ring due to their larger size (scalebar = 100 μm). The graph shows that the higher cell density seeding yields thicker rings which appear to reach a stable thickness faster compared to the lower cell density ones. The individual cells can be visible seen right after they are seeded into the mold. C) the cells have begun to self-assemble into a ring shape however still some cells on the outer edges can be distinguished. D) 18th hour for the low cell density case; a visibly clear ring has been formed and the individual cells can no longer be seen, at this point the cells have assembled into their ring structure but continued to contract until they reach the final thickness. E) The final thickness of the ring shown at day 2, this thickness was maintained until the end of the culture period.

3.2.3. Patterns of Self Assembly in Control and Patient Cases

After the seeding conditions were optimized, patient cells were seeded following the same procedure. The kinetics of ring formation was also used to observe any difference in the contraction behavior between the patient and control cell lines. The patient cells showed a clumping behavior during self-assembly which formed temporary gaps along the ring width. The observed gaps are labeled in red in Figure 3.6 (A), this behavior was consistently observed in all 3 patient lines and none of the control lines. The gaps formed right before the cells contracted into an opaque ring structure. While these gaps were temporary, and they were not observed in the final rings, the patient lines showed some non-uniformities. The non-uniform self-assembly lead to a non-uniform final ring.

Some regions were thinner and some showed thick bulb like regions. Often, when the rings from the patient lines broke after 3-4 days in culture, the breakages were from these thinned out regions. The images of the resultant rings after 8 days of culture are shown in Figure 3.7.

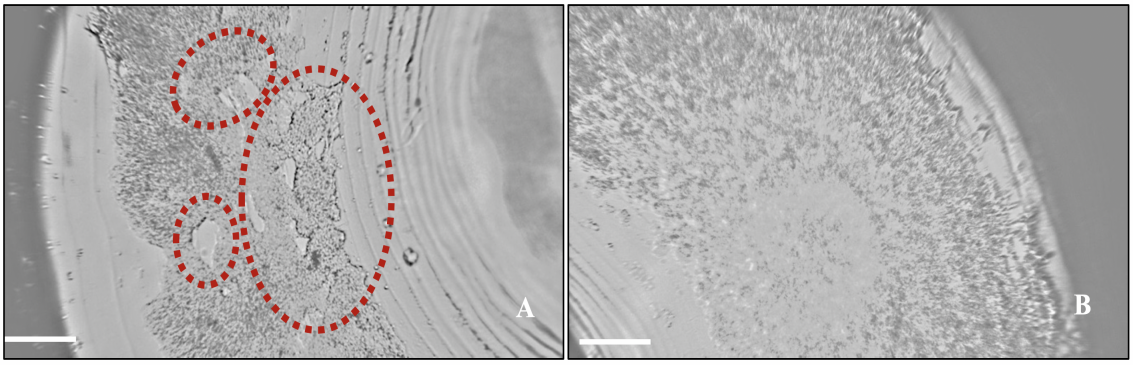

Figure 3.6: The images of a patient and a control ring taken at the same time point (12h). A) The ring formation process for P2 cell line shows multiple gaps appearing along the thickness of the ring and clumping of cells in several regions. B) A control cell line during ring formation appear to have a more spread out distribution of cells throughout the well. (scalebar = 100μm)The resultant rings from these cell lines show a nonuniform and a thin ring for P2 and a uniform ring for the control. The corresponding rings are shown in Figure 3.7 below.

3.2.4. Incidence of Ring Failure and Non-Uniformity in Control and Patient Cases

The incidence of ring formation differed between patient and control cases as well. More rings failed to form or break before the end of the culture period in patient cases compared with controls. All patient rings formed consistently thinner rings compared with the controls; P2 and P3 rings were too thin and nonuniform to be removed from the molds and placed on a tensile testing machine for any mechanical testing. However, it was possible to obtain robust and uniform yet thin rings from P1. Representative images of the rings from each cell line is shown in Figure 3.7 where the thickness and uniformity of the rings can be seen. The numbers of all seeded and formed rings from all cell lines are presented in the Table 3.2.

It was possible to seed a higher number of rings from the control lines and P1 since these had a higher cell viability when counted for ring seeding. The number of rings formed includes the rings which were successfully cultured for 8 days. Most breakage relative to the number of seeded rings was observed in P2 while the least was from P1. However, some rings were also broken while removing from the molds due to their non-uniformity. Cell lines P2 and P3 made very fragile rings and non could be removed from the molds without breaking. Of the overall seeded rings 29% Of the patient cases failed while 100% of the control cases survived as a ring until the end of the 8 day culture period.

Table 3.2: The table shows the number of successfully formed rings versus the number of seeded rings. Rings formed represent the number of rings which remained until the end of an 8 day culture period. An extra batch of 5 rings were seeded from the control lines during the cell seeding optimization trials. Additionally, control lines and P1 showed a higher cell viability during cell counting which allowed seeding more rings from these lines.

	Rings Seeded	**Rings Formed**	**Broken During Removal**
P1	10	9	1
P2	8	4	1(the remaining rings were too thin to be removed)
P3	6	4	1(the remaining rings were too thin to be removed)
C1	15	15	1
C2	13	13	0

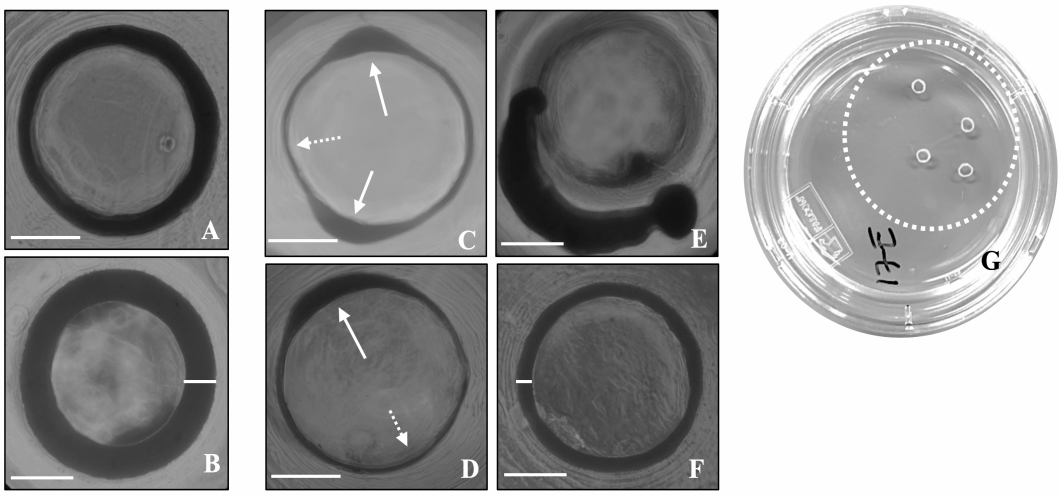

Figure 3.7: Figures on the left A and B show the rings produced by control cell lines while C, D, E and, F are from patient cells. A and B show robust and uniform rings. While C and D, from patients P2 and P3 respectively, show nonuniform rings with bulbs forming in several regions, these rings were very thin on one side and thicker on the other which caused them to be fragile. E shows a prematurely broken ring while F is a ring from P1 cells forming a uniform yet thin ring (scalebar = 1000μm) G) The control rings are indicated with the dotted circle, they were successfully removed from the molds and washed in a petri dish with PBS.

The images shown in Figure 3.7 were taken at the end of 8th day, before the rings were removed. The two control lines all showed uniform and thicker rings which could be removed from the molds without failing as shown in Figure 3.7 (G). As indicated with the white arrows P2 and P3 rings had a non-uniform thickness with bulb like accumulations of cells occurring in some regions. Due to these bulbous formations other regions were much thinner in comparison. These cell lines also showed premature breakage of rings on days 3-4. The rings which failed, broke from these thinned out points, as indicated by white dotted arrows. P1 rings, as shown in Figure 3.7 (F), were uniform in thickness similar to the control lines and most could be removed without breaking, however they were thinner.

3.2.5. Kinetics of Ring Formation for Patient and Control Cases

In order to observe the speed with which different cell lines produce rings, their self-assembly and contraction over the course of 24 hours were measured. At the end of the day it was possible to observe a ring by all cell lines. Differences in cell lines were observed in terms of speed and thickness. The controls, P2 and P3 all completed their self-assembly into the ring structure by the 18th hour time point and maintained a stable thickness afterwards. P1 cell line took longer than 18 hours to assemble into a ring but had formed a stable ring in 24 hours and maintained this thickness. By the end of 24 hours the patient lines contracted into thinner rings compared to the controls, as evident in their final thickness as well.

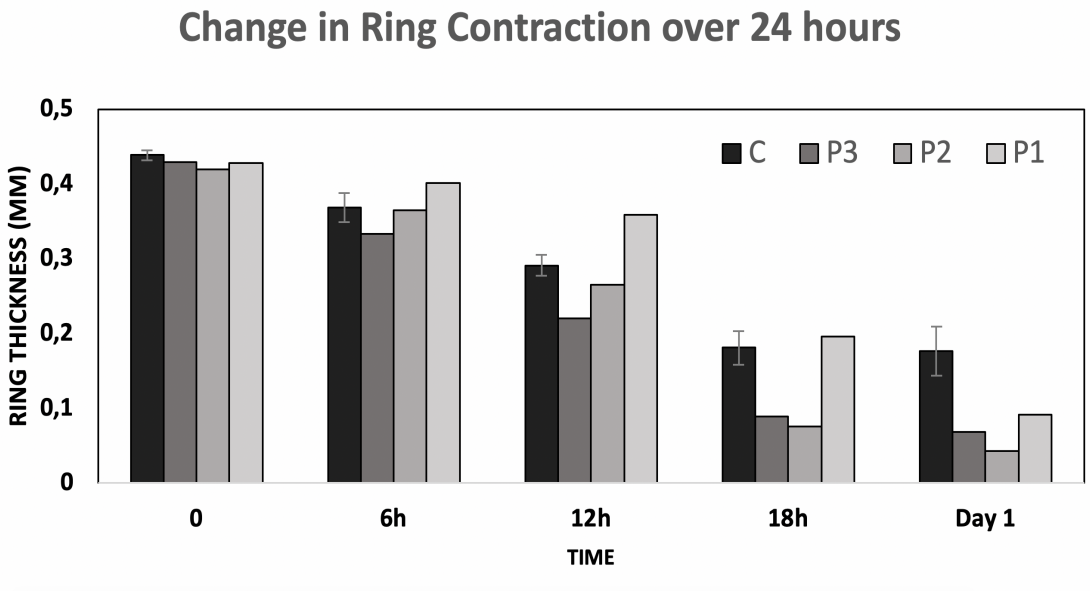

Figure 3.8: The graph shows the change in ring contraction over the course of a day for control and patient cell lines. All patient rings produce thinner rings compared to the 2 control cell lines used. Except for P1 the patient cells seem to follow a similar time span for aggregating into a ring; after the 12h time point C, P2 and P3 appear to assume a more stable thickness while P1 reaches this state after 18h.

3.3. Histology

This section presents the results from the H&E and Picrosirius Red (PSR) stainings. The rings were harvested and stained at the end of day 8. The H&E stainings show the overall morphology of the rings, as well as the distribution and the density of the cells. The H& stains the cell nuclei purple and the cytoplasm pink. Picrosirius Red is a stain specific for collagen, showing the collagen fibers produced by the fibroblasts, their density and distribution. Additionally, these images were used to calculate the ring thickness for each case.

3.3.1. Overall Morphology

The histology images showed that the control rings were tightly packed with cells as seen in Figure 3.9 (B). The overall morphology of the ring showed that there is a uniform cell distribution throughout the ring. The control rings presented a uniform distribution of both cells and collagen fibers throughout their thicknesses as indicated by the black arrows in Figure 3.9. The red collagen fibers were evident along the length of the ring and distributed in a random orientation as shown in Figure 3.9(A). All of the control rings were tightly packed with cells and they were distributed homogeneously throughout the ring. The alignment of the cell nuclei found in the outer edge was observed in all control rings. The cells found in the inner regions showed no preferred orientation. The cell distribution and collagen deposition was homogeneous throughout the ring.

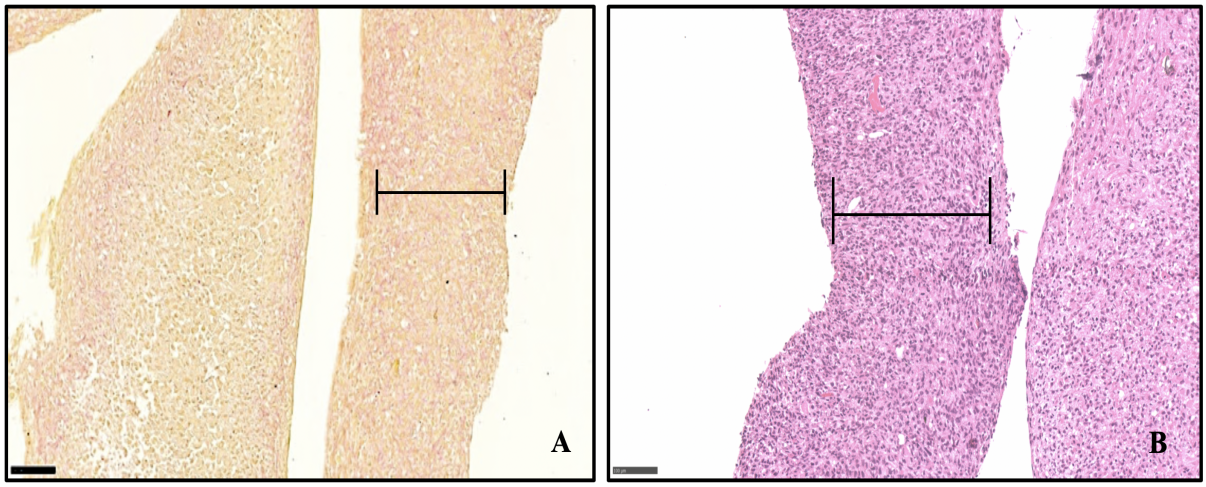

Figure 3.9: A) A representative Picrosirius Red staining of a control ring. The collagen is uniformly deposited throughout the ring as fibers around the densely packed cells. The black arrow shows the span of area where collagen was observed (scalebar = 500μm E) B) The H& staining of the same control ring showed a high cell density and a random orientation of nuclei towards the inner regions with a circumferential alignment towards the outer regions.

However in a control ring which measured thicker compared to the rest (0.78 ± 0.08 mm) there was a lack of nuclei towards the inner regions along the ring thickness, as shown in Figure 3.10. The outer edges which contained more purple stained nuclei are shown with the black arrows in Figure 3.10 (C). Additionally, in a magnified view the cells lining the outer edge, where the ring was in contact with the surrounding culture medium, appeared to be aligned in the circumferential direction of the ring. Similarly, in the PSR stainings the collagen deposition, seen as red fibers around the densely packed cells, appeared around the outer and inner edges of the ring, as indicated by the black arrows in Figure 3.10(D). This trend of cell and collagen focus towards the edges, was not observed in the rest of the control rings which had a mean thickness of 0.55 ± 0.09 mm.

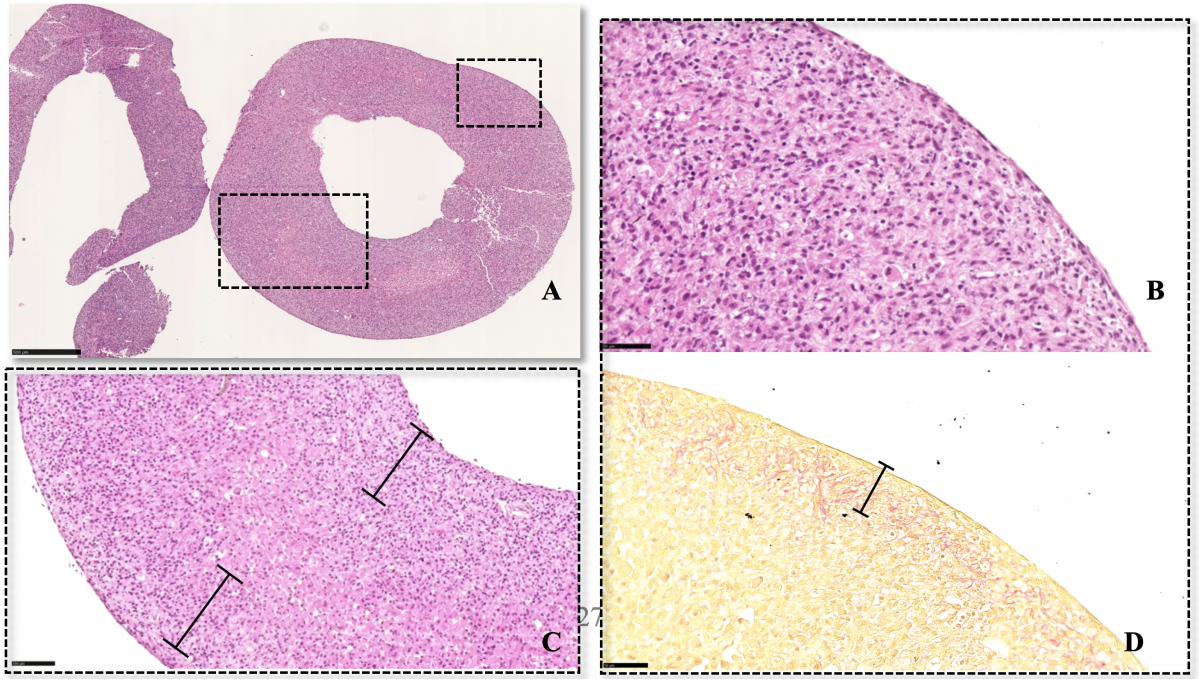

Figure 3.10: A) An overall view of an H&E stained control ring. Purple show nucleus and pink stain cytoplasm. (scalebar = 500μm) B and C are magnified images of the same ring showing the distribution of cells throughout the ring thickness. C) There appears to be more cell nucleus towards the edges of the ring as shown with the black arrows. The inner regions lack cell nuclei which may be indicative of cell death. (scalebar = 100μm) D) shows the same region as B in PSR staining, the collagen is shown as red which appear to be accumulated towards the edges. (scalebar = 50μm)

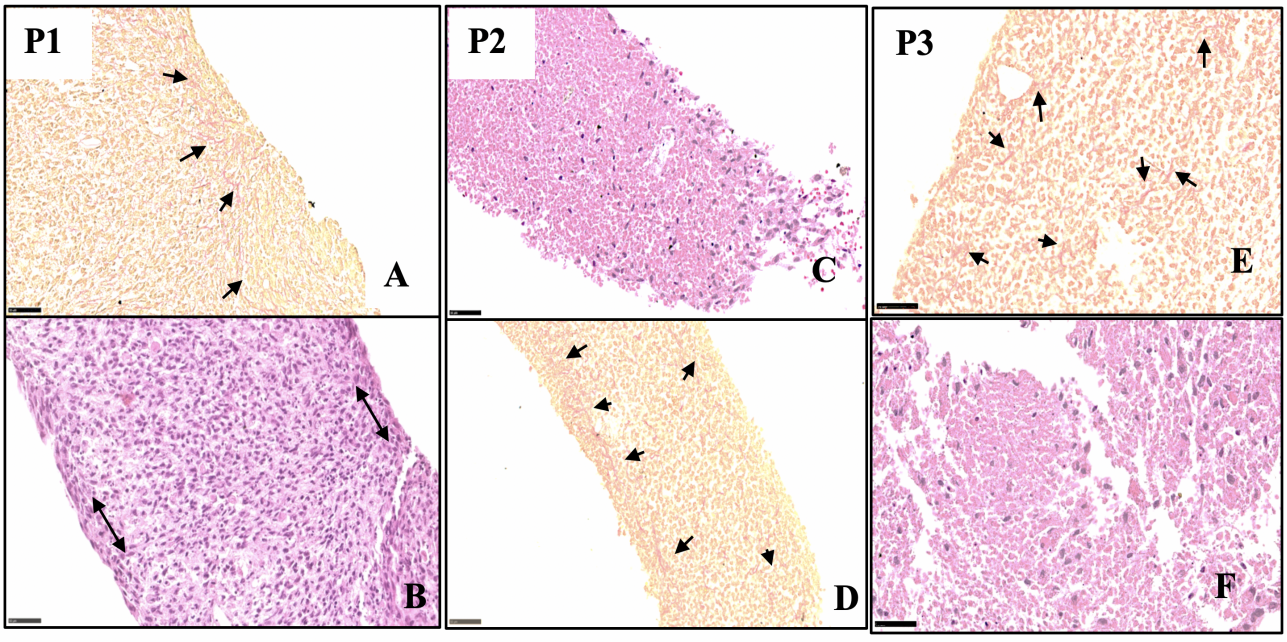

Figure 3.11: The H& and PSR staining of all patient lines, P1, P2 and P3. (scalebar=50μm) In the PSR stainings, collagen appear as red fibers, the area where collagen fibers are focused is indicated with the black arrows. In the H&E stainings, the cell nuclei is dyed as purple their alignment in the circumferential direction is indicated with the black arrows.

Rings from all patient cell lines were similarly stained and qualitatively assessed. These observa-

tions are summarized in the table below, the parameters for investigating the morphology of patient and control rings are the density and distribution of cells and collagen within these rings. P1 rings showed a tightly packed morphology with a homogeneous distribution of cells as seen in Figure 3.11 (A). The cell alignment along the edges which present in control lines, was observed in this case as well (B), similarly the inner regions had no preferred cellular orientation. The PSR staining for P1 showed that there were collagen fibers present throughout the ring however the fibers were more focused towards the outer edges as indicated by the black arrows in Figure 3.11 (A).
P2 rings showed a significant lack of stained nuclei. The H&E stain at a broken region of the ring showed there were a higher number of cells focused in this region. Additionally there was a relatively higher number of nuclei observed around the ring edges. The PSR stain showed a relatively more uniform distribution of collagen fibers as opposed to the cell distribution, as indicated by the black arrows in Figure 3.11 (D). The inner edge of the ring showed denser collagen fiber accumulation compared to the outside. P2 and P3 showed a less packed cell distribution compared to the controls and P1. P3 rings showed a randomly distributed collagen deposition throughout the rings. Similar to P2 there was a lack of nuclei and no orientation could be observed. The rings from P2 and P3 were broken and nonuniform which might be the reason for a lack of observed cellular alignment.

Table 3.3: The table below summarizes the overall morphological observations by the H&E and PSR staining, comparing the individual patient and control cases.

		Cell density	**Cell distribution**
H&E	P1	high	homogeneous
	P2	low	focused on the edges
	P3	low	random-scarce
	C	high	homogeneous
		Collagen density	**Collagen distribution**
PSR	P1	low	homogeneous
	P2	Lower than controls	homogeneous
	P3	Lower than controls	homogeneous
	C	highest	homogeneous

3.3.2. Ring Thickness

Since some rings were not robust enough to be removed from the molds successfully, the final thickness measurements were conducted using the histology images. The final thickness of the patient rings was compared to the controls. Overall, the patient rings (n=6) produced significantly thinner rings compared to the control rings (n=4, $p<0.05$). The Figure 3.12 shows how these groups compare; the mean thickness for control groups were 0.55 ± 0.09 mm while for the patients it was 0.29 ± 0.06 mm. When the thickness of each individual patient ring was calculated the average ring thickness for P1 (n=2) , P2 (n=2) and P3 (n=2) were 0.24 ± 0.06mm, 0.30 ± 0.02mm and 0.35 ± 0.02mm

respectively. Figure 3.12 presents the thickness values of each cell line. At end of the culture period of 8 days, all patient lines consistently produced thinner rings compared to the controls. P1 produced the thinnest rings while P3 and P2 made thicker yet less uniform rings.

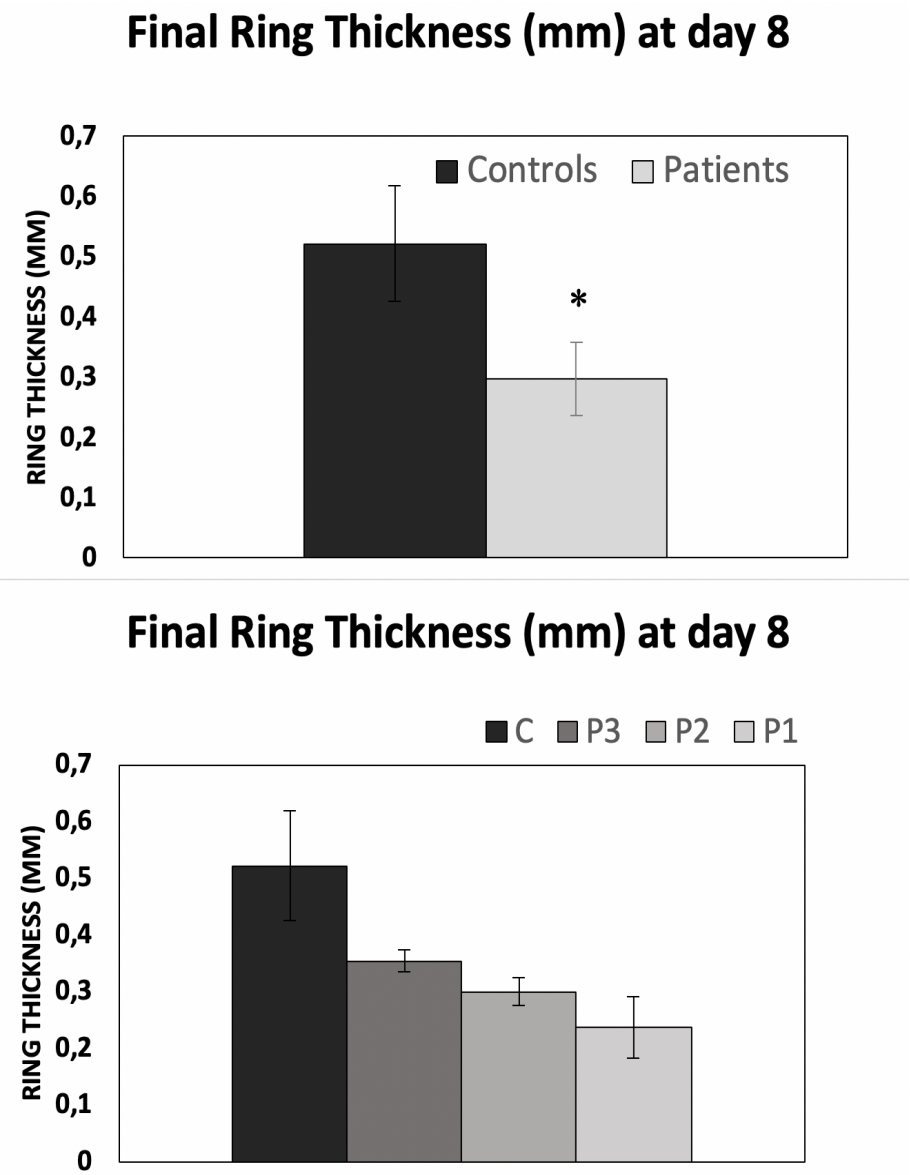

Figure 3.12: The graph on the top compares the thicknesses of the rings produced by control and overall patient lines at the end of the 8 day culture period. The AAA patient rings produced significantly thinner rings compared to the controls ($p < 0.05$). The bottom graph shows the thicknesses of the rings produced by the individual patients; P1, P2 and P3. P1 which has a *COL3A1* null mutation produced the thinnest rings while P2 and P3 were similarly thinner compared to the controls.

3.3.3. Collagen Content

Patients chosen for the ring production system all had genetic variants affecting their collagen production or regulation. P1 had a *COL3A1* null mutation, P2 *COL3A1* missense mutation and P3 had a

TFBR2 mutation. In order to observe whether the effects of these mutations on the collagen synthesis could be observed in this system, the rings were stained for collagen. The stained images were then used to calculate and compare the % area fraction of collagen produced by the different cell lines. Figure 3.13 below show a representative PSR staining of a control and P1 ring. The differences in the collagen amount, stained as red, can be seen in these images. At an initial glance the high amount of red fibers in the case of the control could be seen compared to the patient case. The red fibers appear slightly thicker in the control rings and they seem to be more tightly packed compared to the patient rings. The magnified stained images chosen for this comparison and the collagen area fraction were chosen from at least three points within a ring from the same regions.

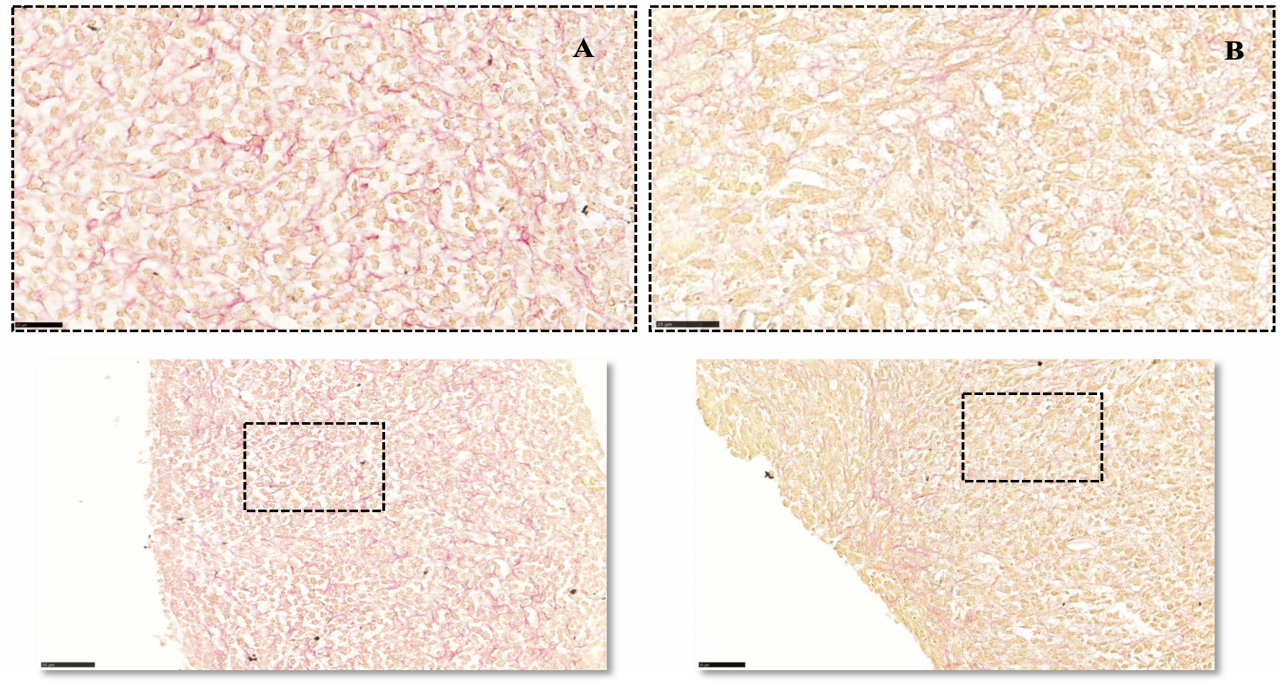

Figure 3.13: A) The red collagen fibers produced by the control cells can be seen. The fibers seem to be oriented in all directions and thicker compared to the P1 (scalebar = 25μm). B) The same magnification as the control ring showing fewer red stained collagen fibers. The fibers appear thinner and similarly oriented in all directions. (scalebar = 50μm).

Using similar histology images from all cell lines the % area fraction of collagen was calculated in ImageJ. First the images were separated into their color channels, identifying the green channel highlights the red stained areas further. Then a threshold value which selects the red stained collagen fibers is set and the area is calculated. Figure 3.14 below shows that the % area of collagen in the overall patient rings were significantly less compared to the control rings. When the % collagen area for each individual patient case is observed, the patient P1 which had a COL3A1 null mutation had the lowest value compared to the rest of the cell lines.

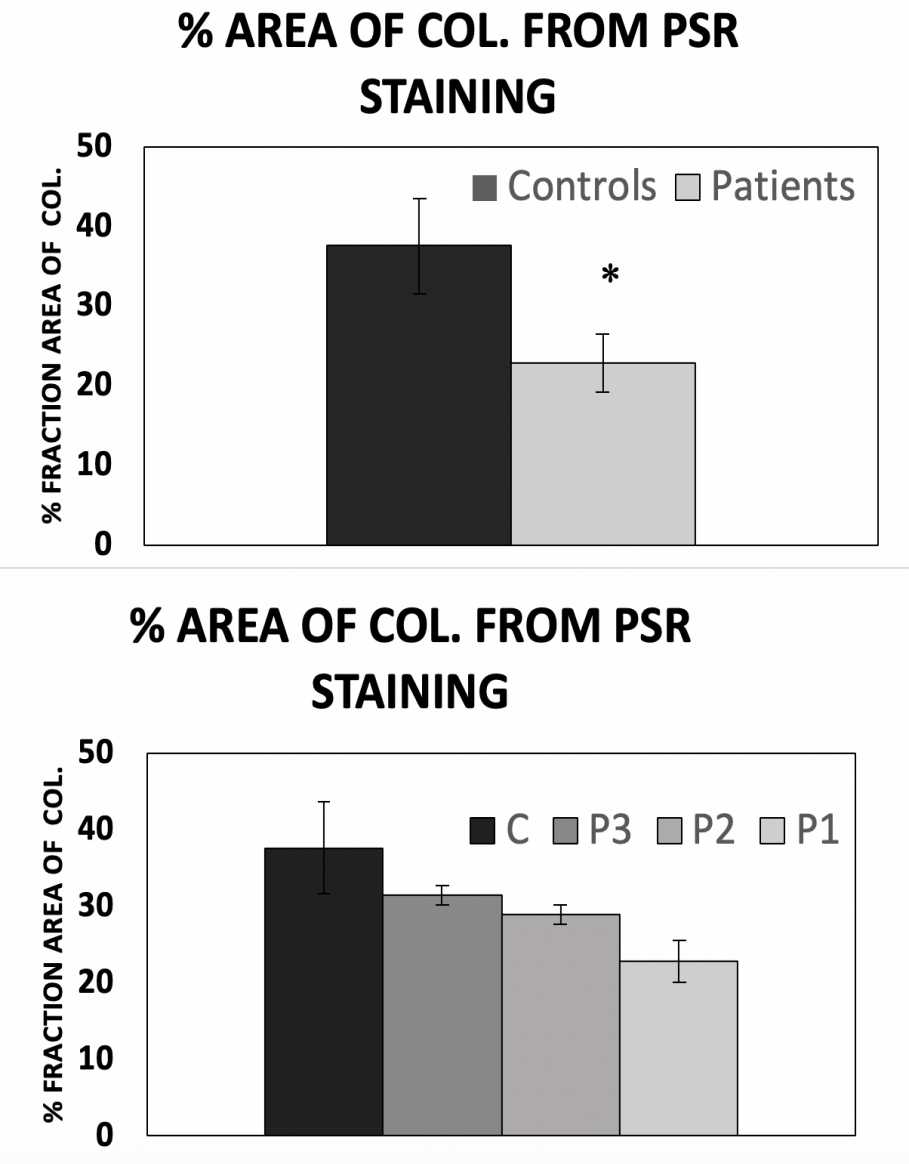

Figure 3.14: The % area fraction of collagen produced by patients lines vs. the control lines are presented in the top graph. The patient rings deposited significantly less collagen compared to the controls ($p < 0.05$). The graph below shows the % area fraction of collagen produced by each cell line. Calculated using the 40X magnified images of the PSR stained rings from each cell line. The area occupied by the red fibers were isolated in an image processing software to calculate their percent area fraction.

3.4. Mechanical Test

The initial plan for the fibroblast rings was after optimizing ring production, the structural and mechanical characterization were to be conducted. While the initially seeded control rings were successfully removed from the molds, the relatively low forces generated by the rings until failure could not be recorded using the existing setup. Additionally, the patient cells did not yield robust enough rings for mechanical testing, while it was possible to remove some of them from the molds, they were too fragile for mounting on the mechanical test setup. Following this trial a more sensitive

load cell of 0.5N was chosen however, further experiments could not be conducted due to the contamination in the cells. Additionally, the fragility of the P2 and P3 cell line rings prevented them from being mounted on the setup.

3.5. Summary of the Results

The cell seeding conditions for cell aggregated tissue rings were optimized for seeding fibroblasts type cells. By using a cell density of 800.000 cell /ring and leaving the cells undisturbed for at least 48 hours and then refreshing the culture medium every other day it was possible culture durable rings in 8 days. The cells self-assembled into a ring shape within the first 18 hours and a visible ring was observed in the culture mold in 24 hours. After optimizing the cell seeding conditions, it was possible to make rings using the patient cell lines as well. The kinetics of ring formation showed differences in behavior and speed for patient and control cell lines. Patient lines took a slightly longer period of time to settle into the ring shape and contract to the final thickness. The number of rings which survived until the end of the culture period also differed between patients and controls. While all rings survived in the cases of control rings, some patient rings broke around 3-4 days of culture time. The final patient rings at the end of 8 days, were significantly thinner and non-uniform, additionally they showed a significantly lowera area fraction of collagen compared to the controls. The mechanical tests could not be performed due to multiple reasons; the initial setup was not sensitive enough to record the force values during the test using control rings. Even though a more sensitive load cell was ordered due to a contamination in the cells, no more sample rings could be prepared. However, the patient rings from 2 cell lines made fragile and nonuniform rings which were not strong enough to be removed from their molds and mounted on the test setup.

4

Discussion

The aim of this project was to design and fabricate a work flow allowing patient cell derived tissue rings to be produced for mechanical and structural characterization in order to observe the effects caused by their genetic variants. A ring culture system was fabricated where self-assembled fibroblast rings from patients and healthy cells could be produced and studied. This method allowed the investigation of the structural differences between the patient and control groups. The initially planned experiments for mechanical tests could not be performed due to a persistent contamination. Additionally the mechanical test setup required the rings to be robust enough for handling. While control groups were so, the patient rings were very fragile hence mechanical data could not be collected. Nevertheless, the study of ring formation process via self-assembly and histology revealed the effects of genetics in patient cases. After further improvements and adjustments, this method could be potentially used as a functional assay for studying the effects of genetic variants of unknown significance.

4.1. Ring Formation

In order to obtain a high throughput ring samples from the fibroblast cells which were available, the cell seeding conditions were optimized. This way a more consistent number of successful rings could be created using a standardized number of cells and a culture media regimen.
Once these conditions were optimized the number of seeded rings and the rings which survived were much more consistent compared to the initial trials. After being able to adjust the culture conditions for fibroblast type healthy control cells, the patient rings were seeded under the same conditions. There were differences in the ring formation behavior, ring morphology and rate of survival between patient and control rings. This could be due to the fact that the patients all had a pathogenic genetic variant which is related to their ECM homeostasis.
Patients P1, P2 and P3 had *COL3A1* null, *COL3A1* missense and a *TGFBR2* mutations respectively.

Their genetic variations had an observable effect on their connective tissue, *COL3A1* null mutation causes the collagen type III to be produced in lower quantities while *COL3A1* missense mutation replaces an amino acid in the alpha chain of the collagen III triple helix. Both of these changes to the collagen in the body results in a loss of function. *TGFBR2* gene codes for the TGFβ- 2 receptor protein. This receptor is a crucial part of the TGFβ signaling pathway which influences cell proliferation, cell growth, motility and cell-ECM interaction.

While studying the ring formation process two stages were observed; the initial self-assembly of the detached cells into a ring shape and its subsequent contraction into a firm ring. In the initial stage, the normally adherent cells can not adhere to the mold surface and therefore they find their closest neighbors and attach. This behavior of the cells could be explained by the need to minimize their surface energy [5]. According to the differential adhesion hypothesis, explaining the phenomena of cellular self-assembly based on thermodynamic laws, cells spontaneously aggregate into a spherical structure in order to minimize their free energy [5]. It is potentially an insight into how fibroblast cells behave in wound healing where they arrive on the wound sight to remodel the ECM. This phenomena is important for aneurysm formation and prognosis as well, since the vessel wall of the aneurysm sight fails to remodel to restore previous structure and function [1, 4].

Studies Gwyther et al. and Wilks et al. describe the process of self-assembly as, contractile type cells proliferating and reaching a high density, and then finding the neighboring ones and adhering to each other [13, 19]. They then contract further making a ring. Later on the cells produce ECM proteins and fibers generating a stronger tissue. The fact that the patient rings broke after they had form rings could indicate that the initial stage of self-assembly is based on cell-cell attachment, which was possible for all cell lines. Napolitano et al., and Czajka et al. also report a similar self-assembly period of 24-48 hours for fibroblast and endothelial cell type rings [17, 20] However, later on, fibroblast begin to produce their own ECM. The genetic variants present in the patient group could have hindered their ability to produce an as robust ECM. The differences in the collagen produced by patient and control groups can also be seen from the histology images. The patient group histology showed a lower % area fraction of collagen, indicating that patient rings deposited less collagen compared to controls.

Another trend which was observed in patient group was while assembling into the ring structure, instead of uniformly attaching and contracting around the central posts, the patient cells formed more clumps of cells in certain regions and gaps lacking cells, right before forming the ring structure. This behavior resulted in nonuniform rings. While a ring which broke during this process could not be observed via time-lapse images, a likely scenario for rings which broke prematurely could be that the rings failed when these gaps that form during self-assembly were too large to close during ring contraction. Additionally, the clumpier regions formed the bulb like structures and caused thinning out other regions of the final rings. The initial non-uniform structure of the rings may have lead to the random distribution of cells and collagen in these rings compared to the controls.

While all patient cell lines managed to form rings, some broke before the end of 8 day culture period and formed nonuniform rings. An explanation for this could be because they were not able to produce healthy ECM which was necessary for holding the ring together and providing mechanical strength. Adebayo et al. showed that the main contribution to the mechanical strength of the

self-assembled rings of smooth muscle cells, came from the ECM as they looked at the differences between the mechanical properties of the decellularized and cellularized tissue rings [16]. Since this mechanical strength was provided by the ECM, an inability to produce efficient ECM fibers could be a source of failure.
In order to overcome the subsequent fragility of the rings effected by inefficient or dysfunctional ECM synthesis, possible ways to improve ECM synthesis and functionality could be looked into. During this study, a standard complete cell culture medium was used for the subculture and the ring culture processes. Based on this, after the cells have contracted and formed a stable ring, the culture medium could be replaced with a supplemented one including growth factors and hormones to promote ECM synthesis. It was possible to make sufficient rings using the standard culture medium however a step further into improving the strength of the rings could be to use a specialized culture medium in promoting ECM producing factors. Growth factors and hormones like TGFβ, epidermal growth factor (EGF), fibroblast growth factor (FGF), and insulin promote ECM synthesis [15]. This could be a potential way to overcome the fragility of the patient rings.
Another factor relating the structural integrity of the rings to the ECM synthesis, was seen in the rings which broke in the earlier periods of the culture. These rings contracted further into a spheroid and lost their shape. However, once the rings were harvested at the end of 8 days these rings maintained their shape. This could be because in 8 days cell produced an ECM which helped maintain their structure when released from the molds. Similarly, Livoti et al. observed the contraction of the rat hepatocyte cell type rings cultured in micro-sized toroid molds, for 10 days and reported that while the width and the lumen diameter changed significantly due to contraction the toroid shape was maintained [21].

4.2. Histology

The histology was used to observe the overall morphology of the rings, compare the ring thickness and the collagen content between patient and control cases. The cell density was low in two of the patient cases (P2 and P3), these were also the rings which showed non-uniform ring formation and ring breakage. The lack of stained nuclei could indicate a higher cell death which could be a reason for more fragile rings. The directional alignment of the nuclei at the outer edges of the rings, where the tissue is in contact with the culture medium, was similarly observed in Gwyther et al. and Czajka et al.[13, 20]. Gwyther et al. report that this alignment was more pronounced when the rings were cultured for a longer period [13].
The ring thicknesses of patient and control groups were compared and a significant difference was observed. The ring thicknesses were also measured based on the individual patients with different genetic variations, the sample size was not enough to conclude a significant difference however P1 formed the thinnest rings, while P2 and P3 were still thinner compared to the control group. The differences in ring thickness could again be attributed to the genetic component which influences the cells ability to produce collagen fibers. P1 had a *COL3A1* null mutation which causes the patient to produce less collagen III, this might be the reason for its thinner structure. Mutations in *COL3A1*

are associated with Ehlers-Danlos Syndrome and mutations in *TGFBR2* are associated with Loeys-Dietz. Patients diagnosed with these syndrome often have thin and translucent skin and are prone to abnormalities in their blood vessels [22, 23].
The 8 day culture period was enough to obtain robust rings which showed production of ECM proteins. While this study focused on the production of collagen using the PSR stainings, according to Czajka et al., other ECM proteins like fibrin and laminin were also produced by fibroblasts within 3 days of ring culture. Using the PSR stainings the % area fraction of collagen for the patient and control cases was measured. The patient group produced significantly less collagen compared to the control group and P1 was the patient showing the lowest amount of % area fraction of collagen. The thickness measurements and the collagen area measurements concur each other. This strengthens the theory that the ring thickness is influenced by the amount of ECM produced. All rings started out with the same initial number of cells, and the rings which were thinner, produced lower amounts of collagen likely caused by their genetic conditions. Another influence over the ring thickness could be cell proliferation; in 2 of the patient cases, P2 and P3, there was a lack of nuclei compared to the control cases. This could indicate cell death or an inability of further cell proliferation which could influence ring thickness as well. However, the thinnest rings were observed in P1, which showed a denser nuclei presence, although the sample size was not large enough to declare a significant difference in ring thickness.
A possible confirmation that this method could be used for observing functional affects of genetic variations may be that this thin skin feature was similarly present in the significantly thinner rings produced by these patient fibroblasts. In order to study the collagen fibers produced by patient cells further imaging techniques like Scanning electron microscopy (SEM) and Transmission electron microscopy (TEM) could be used to investigate the structural differences on a closer level. TEM imaging is being used to investigate the quality of collagen in patient skin biopsies who have connective tissue disorders like Ehlers-Danlos Syndrome [22]. A possible approach to validate the ability of this method in mimicking in vitro ECM could be to compare the TEM images of collagen in the ring constructs with these biopsy images.

4.3. Mechanical Test

The initially planned mechanical tests were to be conducted as described in Gwyther et al. [13]. The control rings could be removed from their molds and handled for further testing however this was not the case for patient rings. The patient rings which were not robust enough for testing, could have been so due to their lower thickness, lower collagen content or possible due to the lower amount of nuclei observed in H&E stainings.
While other studies were able to produce rings from SMCs and MSCs that were strong enough to be handled and mounted on a test setup, the fibroblast rings were more fragile and elastic compared to what is reported in these studies [13, 16, 18]. To overcome this, Winston et al. used a similar culture setup to produce rings using collagen gels and fibroblasts, instead of self-assembly of fibroblasts [14]. This approach help produce robust rings, however the collagen gel mechanical properties

could also influence the measured effects. Another approach could be to co-culture of SMCs, MSCs or endothelial cells with fibroblasts [20]. Czajka et al. showed that self-assembled rings from the co-cultures of fibroblasts and endothelial cells were stronger compared to fibroblast cultures alone [20]. This, could be an alternate approach to increase the strength and integrity of tissue rings without a need for a scaffold material. Co-culture methods could provide a support and a more accurate representation of a vascular wall since the intima layer consists of endothelial cells. As mentioned above another possible solution could be to supplement the culture media with factors stimulating the ECM production for a stronger construct.

In addition to the fragility of the rings which made it difficult to conduct mechanical testing, there were differences in the mechanical testing setup used in this study compared to similar studies. The studies which used self-assembled rings of different dimensions and cell types utilized a standard tensile testing machine where a more sensitive load cells of 1N and 0.5N were used. Additionally, these setups contained of a housing unit for the load cell, minimizing environmental interference while recording. Our in-house built setup left the load cell of 2.5N exposed which potentially increased the amount of noise recorded from the surroundings.

While ring tensile testing appear as an ideal option in this setup due to their ring-shaped structure ability to test bulk material properties, other mechanical tests like nano-indentation techniques and Atomic force microscopy (AFM) could be used for mechanical characterization, these require less sample material and could be used for measuring smaller scale forces [24]. However these measure the mechanical properties on smaller a local scale and have their own limitations [24].

While it would have been interesting to be able to mechanically characterize the tissue rings based on the genetic variation effects, it was not possible to do so with the designed system. It was difficult to generate self-assembled rings from all cell lines which were suitable for mechanical testing.

5

Conclusion

The motivation behind this study was to develop a functional assay for investigating the effects of variants on the aneurysm genes that are currently of unknown significance by using patient cells. A scaffold-free, self-assembly ring shaped cell culture model was used in order to characterize the process of self assembly and their structural and mechanical properties. The aims of the study were to 1) design and fabricate the cell culture molds system, 2) adjusting the culture conditions for fibroblast rings and 3) the characterization of these rings.
The self-assembly ring culture molds were successfully fabricated, additionally the in-house tensile testing machine was modified to allow for a ring tensile testing setup. After adjusting the optimum cell seeding conditions, tissue rings from all desired cell lines were successfully formed. The kinetics of ring formation showed differences in behavior and speed for patient and control cell lines. Patient lines took longer to settle into the ring shape and contract to the final thickness. While all rings survived in the cases of control rings, some patient rings broke around 3-4 days of culture time. The final patient rings at the end of 8 days, were significantly thinner and non-uniform, additionally they showed a significantly lower area fraction of collagen compared to the controls. The mechanical characterization of the rings could not be conducted due to multiple reasons; the initial setup was not sensitive enough to distinguish the forces generated by the tissue rings and the patient rings were too fragile to be mounted on the tensile testing machine. However, it was possible to identify the structural differences between the patient and control cases which were expected to be present due to the pathogenic variants in the aneurysm genes of these patients.

5.1. Limitations

The major limitation for this study was the low number of samples. The experiments could not be repeated enough times to show a significant difference between the each patient line with a genetic variation. Additionally despite the results showing structural differences between the patient and

the control groups these could not be related to the mechanical properties. With a higher number of samples and time to conduct further experiments investigating the collagen production and signaling mechanisms in these rings further insight could be obtained about these patients conditions. In the scope of this study patients with pathogenic variants were chosen to make sure there was an effect to be measured by this model. In the future patients with variants of unknown significance should be chosen to validate the ability of the setup to test functional effects. The fibroblasts used in this study were collected from the skin biopsies, although these rings were able to show a difference in behavior, a possible way to improve this model could be to use vascular fibroblasts since cells could behave differently based on where they are found in the body [25].

5.2. Future Recommendations

The following recommendations could improve and support the results from this study:

1. In order to further characterize the ring formation process in more detail, RNA sequencing in stages of self-assembly could be conducted. This could help reveal the cellular mechanisms which play a role in self-assembly through gene expressions and how they change for the patient cases.

2. The experiments from this study should be repeated using a larger sample size and more patients in order to verify the results from this study.

3. Patients with variants of unknown significance should be chosen to validate the ability of the setup to test functional effects.

4. A microscope with time-lapse imaging capabilities that is able to view the entire mold area for recording the full rings during formation could help understand the formation of non-uniformities within the rings

5. An ECM synthesis promoting culture medium could be used after ring formation in order to produce more robust rings.

6. Immuno-stainings specific to the targeted protein or biological molecule that the genetic variant is likely affected could be targeted and stained for a more accurate understanding of the resultant effect.

7. A more sensitive mechanical testing device or load cell could be opted to record the lower scale forces produced by the tissue rings. Alternatively, if the rings are not eligible for tensile testing, compression or indentations tests could be preferred.

8. TEM imaging could be used to investigate the effect of the disease on the collagen on a fibrillar level and its orientation.

Bibliography

[1] S. A. O'Leary, D. A. Healey, E. G. Kavanagh, M. T. Walsh, T. M. McGloughlin, and B. J. Doyle. The Biaxial Biomechanical Behavior of Abdominal Aortic Aneurysm Tissue. *Annals of Biomedical Engineering*, 42(12):2440–2450, 2014.

[2] R. B. Zamaneh Kassiri. Extracellular Matrix Remodelling and Abdominal Aortic Aneurysm. *Journal of Clinical & Experimental Cardiology*, 04(08), 2013.

[3] Q. Xu, M. Mayr, M. Jahangiri, A. Saje, A. Smith, A. Didangelos, K. Mandal, and X. Yin. Extracellular Matrix Composition and Remodeling in Human Abdominal Aortic Aneurysms: A Proteomics Approach. *Molecular & Cellular Proteomics*, 10(8):M111.008128, 2011.

[4] J. H. N. Lindeman, B. A. Ashcroft, J.-W. M. Beenakker, M. van Es, N. B. R. Koekkoek, F. A. Prins, J. F. Tielemans, H. Abdul-Hussien, R. A. Bank, and T. H. Oosterkamp. Distinct defects in collagen microarchitecture underlie vessel-wall failure in advanced abdominal aneurysms and aneurysms in Marfan syndrome. *Proceedings of the National Academy of Sciences*, 107(2):862–865, 2009.

[5] K. A. Athanasiou, R. Eswaramoorthy, P. Hadidi, J. C. Hu, and O. S. Avenue. Self-Organization and the Self-Assembling Process in Tissue Engineering. *HHS Public Access*, pages 115–136, 2015.

[6] F. Tanios, M. W. Gee, J. Pelisek, S. Kehl, J. Biehler, V. Grabher-Meier, W. A. Wall, H. H. Eckstein, and C. Reeps. Interaction of Biomechanics with Extracellular Matrix Components in Abdominal Aortic Aneurysm Wall. *European Journal of Vascular and Endovascular Surgery*, 50(2):167–174, 2015.

[7] E. E. Joviliano, M. S. Ribeiro, and E. J. R. Tenorio. MicroRNAs and Current Concepts on the Pathogenesis of Abdominal Aortic Aneurysm. *Brazilian Journal of Cardiovascular Surgery*, (June), 2017.

[8] P. Berillis. The Role of Collagen in the Aorta's Structure. *The Open Circulation and Vascular Journal*, 6(1):1–8, 2013.

[9] M. J. Chow, R. Turcotte, C. P. Lin, and Y. Zhang. Arterial extracellular matrix: A mechanobiological study of the contributions and interactions of elastin and collagen. *Biophysical Journal*, 106(12):2684–2692, 2014.

[10] A. Pinard, G. T. Jones, and D. M. Milewicz. Genetics of Thoracic and Abdominal Aortic Diseases. 124(4):588–606, 2019.

[11] I. Hinterseher, G. Tromp, and H. Kuivaniemi. Genes and Abdominal Aortic Aneurysm Irene. *Annuals Vasc Surg*, 25(3):388–412, 2012.

[12] K. M. V. D. Luijtgaarden, D. Heijsman, and A. Maugeri. First genetic analysis of aneurysm genes in familial and sporadic abdominal aortic aneurysm. *Human Genetics*, 134(8):881–893, 2015.

[13] T. A. Gwyther, J. Z. Hu, A. G. Christakis, J. K. Skorinko, S. M. Shaw, K. L. Billiar, and M. W. Rolle. Engineered Vascular Tissue Fabricated from Aggregated Smooth Muscle Cells. *Cells Tissues Organs*, 01609(194):13–24, 2011.

[14] T. S. Winston, K. Suddhapas, C. Wang, R. Ramos, P. Soman, and Z. Ma. Serum-Free Manufacturing of Mesenchymal Stem Cell Tissue Rings Using Human-Induced Pluripotent Stem Cells. *Stem Cells International*, 2019:11, 2019.

[15] J.-E. W. Ahlfors and K. L. Billiar. Biomechanical and biochemical characteristics of a human fibroblast-produced and remodeled matrix. *BIOMATERIALS*, 28(13):2183–2191, 2007.

[16] O. Adebayo, T. A. Gwyther, J. Z. Hu, K. L. Billiar, and W. Marsha. Self-assembled smooth muscle cell tissue rings exhibit greater tensile strength than cell-seeded fibrin or collagen gel rings. *J Biomed Mater Res*, 101(2):428–437, 2014.

[17] J. P. Napolitano, Anthony P. , Chai, Peter M.S., Dean, Dylan B.A, Morgan. Dynamics of Self-Assembly of Complex Cellular Aggregates on Micromolded Nonadhesive Hydrogels. *Tissue Engineering*, 13(8), 2007.

[18] H. A. Strobel, E. L. Calamari, B. Alphonse, T. A. Hookway, and M. W. Rolle. Fabrication of Custom Agarose Wells for Cell Seeding and Tissue Ring Self- assembly Using 3D-Printed Molds. *Journal of visualized experiments : JoVE*, 134(e56618):3–9, 2018.

[19] B. T. Wilks, E. B. Evans, M. N. Nakhla, and J. R. Morgan. Directing fibroblast self-assembly to fabricate highly-aligned , collagen- rich matrices. *Acta Biomaterialia*, 81:70–79, 2018.

[20] C. A. Czajka and C. J. Drake. Self-Assembly of Prevascular Tissues from Endothelial and Fibroblast Cells Under Scaffold-Free, Nonadherent Conditions. *Tissue Eng Part A*, 21:277–287, 2015.

[21] C. M. Livoti and J. R. Morgan. Self-Assembly and Tissue Fusion of Toroid-Shaped Minimal Building Units. *Tissue Eng Part A*, 16(6), 2010.

[22] C. Angwin, A. F. Brady, M. Colombi, D. J. P. Ferguson, R. Pollitt, F. M. Pope, M. Ritelli, S. Symoens, N. Ghali, and F. S. V. Dijk. Absence of Collagen Flowers on Electron Microscopy and Identification of (Likely) Pathogenic COL5A1 Variants in Two Patients. *genes*, 10(762):1–8, 2019.

[23] D. M. Milewicz. MicroRNAs, fibrotic remodeling, and aortic aneurysms. *J Clin Invest.*, 122(2):490–493, 2012.

[24] D. Sicard, L. Fredenburgh, and D. Tschumperlin. Measured pulmonary arterial tissue stiffness is highly sensitive to AFM indenter dimensions. *J Mech Behav Biomed Mater*, 74:118–127, 2017.

[25] M. D. Lynch and F. M. Watt. Fibroblast heterogeneity : implications for human disease. *J Clin Invest.*, 128(1):26–35, 2018.

List of Figures

List of Tables